MOLECULAR DYNAMICS SIMULATION STUDY OF FINITE-TIME THERMODYNAMICS OF A HEAT ENGINE

By

KUMNEGER TADELE

SUBMITTED IN PARTIAL FULFILLMENT OF THE
REQUIREMENTS FOR THE DEGREE OF
DOCTOR OF PHILOSOPHY
AT
ADDIS ABABA UNIVERSITY
ADDIS ABABA, ETHIOPIA
APRIL 2014

ADDIS ABABA UNIVERSITY
DEPARTMENT OF
PHYSICS

The undersigned hereby certify that they have read and recommend to the Faculty of Graduate Studies for acceptance a thesis entitled " **MOLECULAR DYNAMICS SIMULATION STUDY OF FINITE-TIME THERMODYNAMICS OF A HEAT ENGINE** " by **KUMNEGER TADELE** in partial fulfillment of the requirements for the degree of **Doctor of Philosophy**.

Dated: APRIL 2014

External Examiner: _____
x

Research Supervisor: _____
Dr. Mulugeta Bekele,Dr. Tatek Yergou

Examing Committee: _____
y

_____
z

ADDIS ABABA UNIVERSITY

Date: **APRIL 2014**

Author: **KUMNEGER TADELE**

Title: **MOLECULAR DYNAMICS SIMULATION STUDY OF FINITE-TIME THERMODYNAMICS OF A HEAT ENGINE**

Department: **Physics**

Degree: **Ph.D.** Convocation: **APRIL** Year: **2014**

Permission is herewith granted to Addis Ababa university to circulate and to have copied for non-commercial purposes, at its discretion, the above title upon the request of individuals or institutions.

Signature of Author

Table of Contents

List of Tables

List of Figures

Abstract

The upper limit for efficiency of a heat engine is thermal efficiency of a reversible Carnot cycle, also called Carnot efficiency, η_C. Since a heat engine working at Carnot efficiency delivers zero power with in finite time, the notion of extracting maximum possible power output per cycle has been introduced. As a consequence the upper limit for efficiency at maximum power of a heat engine, called Curzon-Ahlborn efficiency, η_{CA}, is defined. Due to the need of providing a sustainable supply of energy and to strong concerns about the environmental impact of the combustion of fossil fuels, performance efficiency of a heat engine remains a major problem in thermodynamics. In this work we study the performance analyis of a heat engine where real gas is used as a working substance of the heat engine. The performance analysis is conducted through studying the cyclic thermodynamic process in the working substance of an endoreversible heat engine.

We perform a classical molecular dynamics simulation study of a heat engine operating between two heat reservoirs and performing a Carnot-like cycle in a finite time over a wide range of process rates. The heat engine is modeled to use real gas as the working substance where we have used Lennard-Jones potential to consider the intermolecular interaction in the working gas. The piston speed and temperature ratio of cold and hot heat reservoirs are used as control parameters whereas efficiency and power output per cycle are variable quantities of the engine. The variation of these dependent variables as a function of the independent parameters is studied for two cases; when the piston moves with uniform speed throughout the cycle and when it moves with constant but unequal speed on the four branches of the cycle. It is shown that the efficiency of the Carnot-like engine increases for a slower process rate but at the cost of power output. We also compute maximum efficiency and efficiency at maximum power of the engine model considered and the obtained result is in a good agreement with Carnot efficiency and Curzon-Ahlborn efficiency respectively for the later case. It is also shown that the efficiency of the engine

highly increases when the cycle involves instant adiabatic process. Finally we determine optimum values for efficiency and power output per cycle and the corresponding process rate at which these values are attained where we use unified optimization criterion (Ω criterion) to optimize between efficiency and power.

Acknowledgements

I would like to express my sincere gratitude to my supervisors Dr. Mulugeta Bekele and Dr. Tatek Yergou for their unlimited support, guidance, advice, and constructive suggestions and comments.

I am grateful to all my families especially to my parents Tadele Gemechu and Aregash Demessa for their support, patience and *love*. Their continual encouragement has been very helpful.

I would like to thank Dire-Dawa University for the sponsership they granted me to join the school of Graduate studies and the financial support. I am also thankful to Addis Ababa University in general and Department of Physics in particular for the facilities provided and financial support.

I am thankful to all my friends and colleagues for their motivation, cooperation, very useful discusions and for all the funs we have had.

Addis Ababa, Ethiopia Kumneger Tadele
April, 2014

Chapter 1

Introduction

The fundamental limits that thermodynamics imposes on the efficiency of thermal machines is a central issue in physics. This is due to the highly increasing demand of energy in the world and to strong concerns about the environmental impact of the combustion of fossil fuels. A heat engine operating between two reserviors at temperatures T_c and T_h with a special type of theoretical cycle, Carnot cycle, is called a Carnot engine. The efficiency of a Carnot engine, usually called Carnot efficiency, is the upper bound for efficiency of any thermodynamic heat engine and can be obtained for a quasistatic process which requires infinite time and therefore the extracted power reduces to zero. For practical purposes however, real heat engine becomes usefull when it can produce finite amount of power and not just work. As a consequence one usually seeks maximum efficiency at non zero power, or even maximum output power. Hence the notion of efficiency at maximum power has been introduced. An upper bound for efficiency at maximum power is determined by Curzon and Ahlborn and hence termed as Curzon-Ahlborn efficiency.

In Carnot engine, a working gas absorbs an amount of heat H_1 as it expands isothermally from its initial volume V_1 to a larger volume V_2 while in contact with an external heat reservior at temperature T_h. The gas is then adiabatically expands to V_3 and hence cooled to a lower temperature T_c. At this temperature it is compressed isothermally to a volume V_4 while rejecting an amount of heat H_2 to an external heat sink at temperature T_c. Finally, it is further compressed adiabatically until it reassumes its initial volume V_1

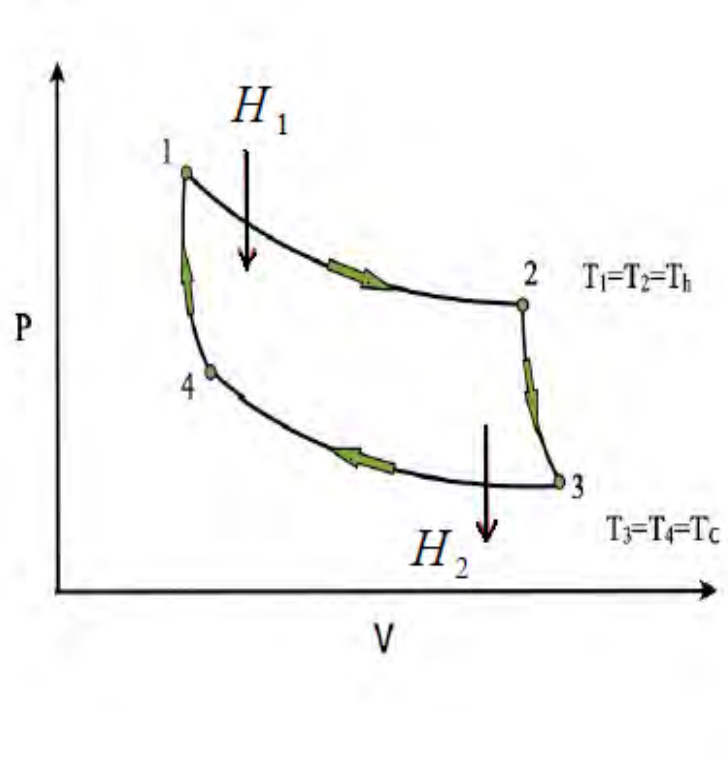

Figure 1.1: Pressure-Volume diagram of Carnot-like heat engine

and temperature T_h. Here V_i represents the volume of the sytem at point i shown in Fig. 1.1, i = 1, 2, 3 and 4. $H_1(H_2)$ is the amount of heat absorbed(exhuasted) by the engine. Because the work that must be expended in the two compressions is less than the work gained in the two expansions, the net work done during a full cycle is positive and is given by $W = H_1 - H_2$. The fraction of the recieved heat H_1 that is transformed into work, $\eta = W/H_1 = 1 - H_2/H_1$, defines the efficiency of a thermodynamic engine. According to the First and Second Laws of thermodynamics, the maximum efficiency of an engine that transfers heat from a heat source at temperature T_h to a heat sink at temperature T_c is given by

$$\eta_c = 1 - T_c/T_h, \tag{1.0.1}$$

which is called Carnot efficiency. This value is achieved only by a quasi-static process in which the working gas passes infinitely slowly through a continuous sequence of equilibrium states [1]. The Carnot efficiency can only be achieved when the engine works

infinitely slowly; conversely, as the speed of the thermodynamic cycle of the engine increases, its conversion efficiency decreases. For very fast cycles the efficiency even reduces to zero. This condition implies that Carnot engines are idealizations from which all real thermodynamic engines will more or less deviate.

Carnot efficiency is the upper limit for efficiency of any heat engine. However, to obtain such a maximum efficiency, it takes an infinite amount of time to extract a finite amount of work. This means Carnot engines deliver zero power with in finite time and are practically unimportant. From a theoretical as well as a practical point of view, only models of irreversible heat engines must be considered to address the central points of causality and system evolution. The dependence of the engines efficiency, η, and power output, P, on the working conditions is the direct consequence of this introduction of irreversibilities in heat engine models. The out put power of a heat engine, the ratio of work done by the engine to the cycle time, will vanish when the cycle time is too long. On the contraty, if the process speed increases too much, irreversibilities become preponderant and power vanishes again. Hence it is customary to deal with the variety of working conditions between these two extremes and searching for a working condition which leads to a power maximization. Following Carnot's insight and since the industrial revolution, a lot of studies have been made concerning the efficiency of heat engines. The earliest study of efficiency at maximum power was done by Odum and Pikerton in 1955 [2]. Curzon and Ahlborn calculated the efficiency of an endoreversible heat engine, a thermodynamic engine which undergoes reversible process only in the working substance, that operates at maximum power in 1975 [3], which is first demonstrated by Novikov in 1957 [4, 5]. The same result was also derived by Chambdal in 1957, but by modeling a different thermal conductance between reserviors and working substance [6]. However this result is usually known as Curzon- Ahlborn efficiency, η_{CA}, which, like the Carnot

efficiency, depends only on the temperature of the resorviors and is given by

$$\eta_{CA} = 1 - \sqrt{\frac{T_c}{T_h}}. \tag{1.0.2}$$

The Curzon-Ahlborn efficiency is in good agreement with the real efficiency at maximum power values for most power plants and hence it is considered as a universal upper bound for efficiency at maximum power of heat engines [7, 8]. In the Curzon-Ahlborn engine there is no thermal equilibrium between the working fluid and the heat reserviors at the isothermal branches of the cycle and the adiabatic branches are taken to be instantaneous.

The efficiency of non-ideal Carnot engine (or Carnot-like engine or heat engine operatting with a Carnot-like cycle), a thermodynamic engine which considers different external sources of irreversibility like friction, heat leak, etc., is always less than Carnot efficiency. In the regime between maximum efficiency at zero process speed(quasi-static process), and zero efficiency at the largest possible speed without net energy losses, there exists a process speed at which the power output of the engine becomes maximal. For the case of heat losses only, which is calculated by Curzon and Ahlborn; the corresponding efficiency is given by η_{CA} [3]. Since the new efficiency limit characterized by finite rate, finite duration and finite size was first drived by Novikov and Chambdal simultaneously and rediscovered by Curzon and Ahlborn, the analysis and optimization of all kinds of thermodynamic cycles has made tremendous progress by using finite time thermodynamics (FTT). Traditional thermodynamics is a theory about equilibrium states and about limits on process variables for transformations from one equilibrium state to another. This traditional thermodynamics is extended to FTT to obtain more realistic limits to the performance of real processes and hence FTT deals with processes which have explicit time or rate dependencies [9, 10]. An extension of classical equilibrium thermodynamics to a thermal engines whose operation involve time dependent interation process of the working substance of the engine with the surrounding while excluding possible irrevesibilities with in the working substance is called endoreversible finite time thermodynamics (EFTT).

Endoreversibility, excluding possible irreversibilitie with in the working substance, can be considered for cases in which the internal relaxation time of the working substance is negligibly short as compared to the total time of the cycle [11]. FTT provides an approach to quantify cycles and plant components irreversibilities and thereafter can provide more applicable results for engineering design guidance. Since after its estblishment in the pioneering work of Novikov, Chambdal, and Curzon and Ahlborn, FTT has been used progressively in cycle and power plants performance analysis and start to regulary appear in differnt publications in the field.

H. Feng et.al. used FTT to analyze the performance of an endoreversible Carnot heat engine cycle [12]. In their study they consider a Carnot cycle model with constant but unequal piston speed on the four branches of the cycle. In their study the authors report that the power is related to the efficiency of the cycle η, the isothermal expansion ratio $V^* = \frac{V_2}{V_1} = \frac{V_3}{V_4}$, the cycle period τ and temperature ratio of the heat reserviors $T^* = \frac{T_h}{T_c}$. It is also shown that the ratio of the volume to the rate of change of the volume, the product of piston speed with cross-sectional area of the piston, at the starting point, $\frac{V_2}{u_1}$, where u_1 is change rate of the volume on the first branch, of the cycle affects the power out put. Moreover the power out put increases monotonically when T^* increases provided that either efficiency η or isothermal expansion V^* kept constant, however it decreases monotonically when $\frac{V_2}{u_1}$ increases.

D. C. Agrwal and V. J. Menon used FTT to calculate the cycle time of each branch of a finite speed carnot engine on the assumption of the finite speeds of the piston on the four branches are equal [13]. They used this cycle model to investigate the relation between power and efficiency of a finite speed Carnot engine. A finite power out put produced by an endoreversible Carnot engine operating at constant piston speed can be optimized with respect to isothermal expansion ratio V^* and isothermal temperature ratio T^*, which is a different theory as compared to that of Curzon and Ahlborn where they introduce thermal conductances at the upper and lower isotherms and assume instantaneous adiabatic

branches to produce finite power. Their finding shows that the temperature ratio T^* and the isothermal expansion ratio V^* at maximum dimensionless power are not affected by the finite speed of the piston and initial configuration of the system (P,V,T), though the out put power increases with the piston speed u. Moreover, it is shown that the out put power P increases with in a finite range for η and beyond this range the power decreases. This is because both for too large period τ (too small piston speed) and too small period τ (too large piston speed) the out put power becomes very small, since, in the later case, only small amount of supplied heat can be converted to work.

For endoreversible heat engine, when only friction losses are taken into account the efficiency becomes

$$\eta_E = \frac{1}{2}(1 - \frac{T_c}{T_h}). \tag{1.0.3}$$

If the effect of both heat losses and friction losses are taken into account, the efficiency can vary between a lower limit, η_E, obtained for friction losses only, and an upper limit, η_{CA} , for heat losses only [14]. As reported in reference [14], to obtain the highest possible efficiency, friction losses should be reduced as much as possible. Inclusion of friction losses in the heat engine model leads to obtaining efficiency at maximum power out put which is less than the Curzon-Ahlborn efficiency and it becomes more closer to the observed efficiency of real engines. Thus, generally speaking, besides the irreversibility of finite-rate heat transfer in finite time taken into account in the Curzon-Ahlborn engine, there are also other sources of irreversibility, such as heat leaks, friction losses, dissipative processes inside the working fluid and so on, which influence the performance of heat engine [15]. Working at maximum power leads to substantial amount of the input energy to be wasted. On the contrary, working at maximum efficiency has no practical importance. Hence it is vital to compromise between maximum efficiency and efficiency at maximum power, that means to optimize the efficiency and power of the heat engines.

In reference [3] the authors report about thier consideration of the irreversibility of a linear finite rate heat transfer between the working fluid and its two heat reservoirs,

though it is not the only source of irreversibility in real heat engines. The Curzon-Ahlborn efficiency η_{CA}, which determines the efficiency at maximum power production of heat engines, only affected by the irreversibility of finite rate heat transfer (endoreversible engines), but η_{CA} is not the upper bound of the efficiencies of heat engines. This is conceptually different from the role of the Carnot efficiency η_C which is indeed the upper bound of the efficiencies of all heat engines. Although the efficiencies of real heat engines can not attain the Carnot efficiency, it is possible, and often desirable, for their efficiencies to be larger than their respective maximum power efficiencies. In fact, the maximum power efficiency is the allowable lower bound of the efficiency for a given class of heat engines [16]. In reference [17], M. Esposito et.al. cleared that CA efficiency is an exact property of Carnot machines operating at low, symetric dissipation. They have also put upper and lower boundary for the efficiency of Carnot machines operaring at low, asymetric dissipation. Though it is not an upper or lower bound, CA-efficiency describes the efficiency of actual power plants to a good approximation [3, 11].

The performance analysis of heat engine which involve some irreversibilities has been studied by different scholars using various approaches of power maximization techniques. Another method called entropy generation minimization which combines thermodynamics, heat transfers and fluid flows is introduced by Bejan. The establishment of this technique, also known as FTT, motivates many scholars to work on performance analysis of heat engine, optimization of finite time and finite rate processes and optimization of finite size devices. The optimization criteria used in these studies include power output, thermal efficiency and entropy generation [18-23]. The effect of engine size on the performance analysis is reported in [24] which introduce a new optimization criteria called maximum power density (the ratio of power to the maximum specific volume in the cycle). More efficient optimization criterion called maximum efficient power, which considers both power output and efficiency, has been applied to study a heat engine operating with Carnot-like cycle [25, 26, 27].

G. Mahshewari et.al. suggested a radiative heat engine model which supposed to meet the demands of maintaining air quality standards and diminishing energy resources. They report their theoretical anlysis on the model of internally and externally irreversible radiative heat engine. In this study it is reported that the radiative heat engines designed based up on maximum efficient power optimization criterion is smaller in size and more efficient as compared to the conventional heat engines whose development is suffering from environmental challenges. It is also suggested that the maximum efficient power optimization criterion can be successfully employed in designing ecofriendly external combustion engines in order to develope an engine with enhanced efficiency and smaler size [27]. Schmeidel and Seifert used a stochastic heat engine model to study the performance anlysis of an exoreversible engine, an engine in which all irreversibilities arise only from internal processes. This hypothesis is completely different from the hypothesis used by Curzon and Ahlborn to study endoreversible engine which involve dissipative thermal contacts between the system and heat reserviors, irreversibility due to external process. In this study a new xpression for efficiency at maximum power is derived which is

$$\eta_{p_{max}} = \frac{\eta_c}{2 - \gamma\eta_c} \tag{1.0.4}$$

where γ is a parameter related to the ratio of entropy production at each end of the engine [28]. This approach is extended to low-dissipation heat engines for which a different expression for $\eta_{p_{max}}$ is developed in [29, 30]. Apertet and his co-workers considered both internal and external irreversibilities in their study of performance analysis for a thermoelectric generators, devices which couple ellectric and heat currents [31]. In 2008 G. Aragon-Gonzalez et. al. reported their study about the optimization of power output and efficiency of irreversible Carnot cycle by considering internal temperature ratio and time ratio for the heat exchange as parameters for the optimization [15]. In the same year Y. Izumuda and K. Okuda studied finite-time Carnot cycle of weakly interacting gas and, for the first time, they verified the validity of η_{CA} numerically using MD simulation technique [32]. The impact of non-linear rates of heat transfer on the performance efficiency

of heat engine is also discussed in [33 - 36]. Some other possible sources of irreversibilities like heat leaks and dissipative process inside the working fluid, and their impact on the performance efficiency of heat engine has been reported in different papers [15, 33].

Since the establishment of FTT much work has been carried out for the performance analysis of heat engine and optimization of finite time processes in it. However, as far as we are conserned, no work is reported which consider the possible intermolecular interaction in the working substance of heat engines. Since in most heat engines the working substance is real gas, we believe that it is vital to extend those works for a real gas case where the intermolecular interaction is significant. And hence in this paper we study the performance analysis of a heat engine operating with a Carnot-like cycle between two reserviors where the working substance of the model engine is considered to be real gas. We apply a classical molecular dynamics simulation technique to study the problem and we employ Lennard-Jones potential to consider intermolecular interaction within the working substance. In this work we have used process rate and temperature ratio of the reserviors to be control parameters, and hence the variation of efficiency and power output per cycle as a function of the control parameters are computed. Finally we apply unified optimization criterion to determine optimum values for efficiency and power output per cycle.

This material is organised as follows: In the second chapter the general background of the problem is discussed. In this chapter brief description about heat engine, Carnot cycle, finite time thermodynamics and efficiency at maximum power is presented. Chapter three presents a brief description of molecular dynamics (MD) simulation and techniques used in MD simulation. In the fourth Chapter the model considered to study the problem and some statistical quantities measured from our simulation are discussed. The fifth chapter presents the result obtained for wide range of process rates and different temperature ratios of the reservoirs. Finally the last Chapter devoted to summary and conclusion.

Chapter 2

Background of The Problem

2.1 Heat Engine

The First Law of Thermodynamics is a statement about conservation of energy. It states that change in internal energy in a system can occur as a result of energy transfer in the form of heat or work or both. Although it has many importance in the development of thermodynamics, the first law makes no distinction between processes that occur spontaneously and those that do not. It is the Second Law of Thermodynamics that establish the distinction between processes that do and that do not occur naturally. According to the second law there are processes which proceed in only one direction spontaneously and the reverse process is impossible unless there is some external reinforcing factor. The most important implication of this law, however, is its limitation on the efficiency of a heat engine. The second law states that it is impossible to construct a machine which is capable of continuously converting internal energy completely to other forms of energy in a cyclic process.

Work can be completely converted to heat, as everyday experience with friction attests. However, the reverse is not true; heat cannot be completely transformed into work. This limitation, which is a consequence of the Second Law of Thermodynamics, is best demonstrated by studying the properties of heat engine, which is a device used to convert heat to work or other mechanical form of energy. A heat engine is a system operating in a

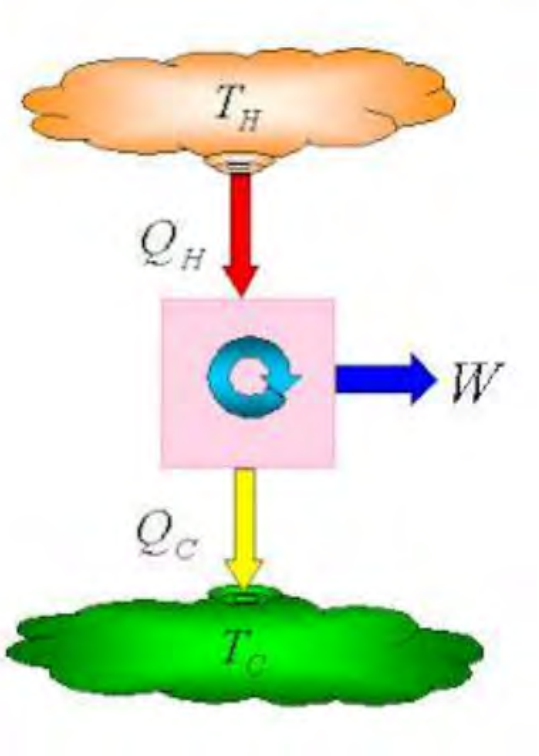

Figure 2.1: Energy flow in heat engine

cycle that receives heat from a high temperature source (called a hot reservoir), produces useful work and exhausts heat to a cold reservior, a low temperature heat sink as shown in Fig. 2.1. Since a device operating in a cycle periodically returns to its initial condition, all state variables of the device return to their initial values once every cycle. A heat engine can continue converting heat energy to useful work for as long as it is attached to the reserviors. However, since the efficiency of conversion must be less than 100 percent, some of the input heat is rejected to a cold reservoir. The reservoirs supply or receive heat without alteration of their temperatures. Heat flow in the reservoirs is reversible whether or not heat flow in the engine is reversible.

Based up on the mechanism of heat production heat engine is catagorized as an internal combustion and external combustion engine. External combustion engine is a type of heat engine where heat is produced by burning the fuel outside the main body of the engine. Steam engine is a typical example for external combustion engine. Steam engine has

thermal efficiency which varies from 0.12 to 0.16, however, this is too much less than what is theoretically estimated. In the case of internal combustion engine however heat is produced by burning the fuel inside the main body of the engine. Petrol engine and diesel engine are internal combustion engines. The thermal efficiency of internal combustion engines varies from 0.26 to 0.4 [37, 38]. The thermodynamics processes in the working substance of internal combustion engine include

- A fuel-air mixture is burned to create a high temperature gas.
- The volume of the gas expands doing work on the environment.
- The exhausted air is expelled to the atmosphere.

Heat engines employ some working substance that is carried through a cyclic thermodynamic process in which the working substance is eventually returned to its initial state. The working substance is most often a fluid or a gas. The working substance moves through many thermodynamic states in a never-ending cyclic process. Heat engines differ considerably from one another, but generally all can be characterized by the following four processes:

- Heat is absorbed isothermally from a high temperature source (hot reservior).
- Work is produced adiabatically.
- Heat is rejected isothermally to a low temperature sink (cold reservior).
- Work is done adiabatically on the working substance to return it to the initial state.

The heat engine can operate in either of two ways:

- as a single device that sequentially moves through the four processes described above, or

- with a fluid flowing through four distinct devices, each assigned to one of the four steps.

There are some fundamental thermodynamic features and limitations of heat engines which arise irrespective of the details of how the engines work. The principal one is a limitation on the possible efficiency of the engine. The efficiency of a heat engine is defined as the ratio of work, W, performed by the engine on the environment to the heat energy, H_1, absorbed by the engine from the source

$$\eta = \frac{W}{H_1} \tag{2.1.1}$$

If we manage to convert all the energy absorbed as heat into work then the efficiency of the engine is unity. This is reasonable in light of conservation of energy. The maximum efficiency we could possibly do in light of the First Law of Thermodynamics is $\eta = 1$. To see this more clearly, recall that a heat engine is by definition a cyclic process. 'Cyclic' means that the engine periodically returns to the same state. The change in internal energy of the system after each cycle is zero. The First Law of Thermodynamics then tells us that the net heat absorbed by the system is the energy transferred out of the system by work. So, just taking account of the First Law of Thermodynamics, we could imagine a cyclic process where heat goes in and an equal amount of work goes out so that $\eta = 1$. However, the Second Law of Thermodynamics implies that an efficiency of unity is not possible. The reason is that the heat transfer of energy in to the engine involves an increase in entropy of the engine [11, 39]. Assuming the heat is absorbed at constant temperature, we have

$$\Delta S \geq \frac{H_1}{T_h} \tag{2.1.2}$$

where T_h is the temperature of the hot reservior or heat source and ΔS is change in entropy of the engine. This entropy must be removed by the time the engine completes one cycle of operation since all observables must return to their original values if the system is

back in its original state. So, whatever entropy increase accompanied the absorption of energy by heat must be undone by the end of the cycle. This removal of entropy requires expelling some heat from the engine. In light of this heat transfer out of the system, conservation of energy tells us that the work done is, at best, the difference of the heat absorbed and the heat expelled

$$W = H_1 - H_2. \tag{2.1.3}$$

Thus the efficiency can be written as

$$\eta = \frac{W}{H_1} = 1 - \frac{H_2}{H_1}. \tag{2.1.4}$$

The Second Law of thermodynamics asserts that after the cyclic process the change in entropy of the system must not decrease. At the end of one engine cycle, the entropy of the engine has not changed. Hence the change in entropy of the environment must be greater than or equal to zero by the second law. But the change in entropy of the environment is given by

$$\Delta S = \Delta S_h + \Delta S_c = -\frac{H_1}{T_h} + \frac{H_2}{T_c} \geq 0 \tag{2.1.5}$$

$$\frac{H_2}{T_c} \geq \frac{H_1}{T_h} \tag{2.1.6}$$

$$\frac{H_2}{H_1} \geq \frac{T_c}{T_h} \tag{2.1.7}$$

where $\Delta S_{h(c)}$ is change in entropy of the hot(cold) heat reservior. The efficiency of the engine is then given by

$$\eta \leq 1 - \frac{T_c}{T_h} \tag{2.1.8}$$

The upper limit on the efficiency of engine is then

$$\eta = 1 - \frac{T_c}{T_h} \tag{2.1.9}$$

To attain this upper limit one must create no net entropy in the environment after each cycle. This can be done via the Carnot cycle, a quasi-static cycle involving four steps of

compression and expansion. This is guaranteed by the fact that the net change in entropy of the engine plus environment is zero. At the end of the Carnot cycle, the entropy change of the engine is zero as well as that of the environment. This means one can get arbitrarily close to the maximum efficiency via the Carnot cycle. The idea of the Carnot cycle is that as you let the engine temperatures approach those of the hot and cold reservoirs the efficiency approaches its maximum. Of course, this means that the engine will work very slowly when it is near its maximum efficiency.

2.2 Carnot Cycle

The Second Law of Thermodynamics states that heat always flows from a hotter to a colder substance, unless some external device is employed. This Law can also be stated as follows: It is impossible to construct an engine, which, operating in a cycle, will produce no effect other than the extraction of heat from a reservoir and the performance of an equivalent amount of work. This statement implies that every engine operating in a cycle which takes in heat from some source or reservoir must deliver some of this heat to a reservoir at a lower temperature. And all heat engines are a consequence of this Law. A special type of heat engine, an ideal engine, is a heat engine that operates with Carnot cycle.

The Carnot cycle was first proposed in 1824, by Sadi Carnot. The interest in the cycle is largely theoretical, as no practical Carnot cycle engine can be built. Nevertheless, it can be shown to be the most efficient cycle possible, so that considerable attention has been given at discovering ways of making the more practical cycles look, as much as possible, like the Carnot cycle. After his discovery, Carnot stated two principles about heat engines:

- The efficiency of an irreversible heat engine is always less than the efficiency of a reversible one operating between the same two reservoirs.

- The efficiencies of all reversible heat engines operating between the same two reservoirs are the same. In other word, no real (irreversible) heat engine operating between two energy reservoirs can be more efficient than a Carnot (reversible) engine operating between the same two reservoirs.

Unfortunately, as a practical engine, the Carnot engine is rather useless. Actually it is impossible to get it to work at all because any real process is not perfectly reversible. Still, in principle at least, this is the most efficient engine you can possibly make, which makes it very useful.

The Carnot cycle is an ideal thermodynamic cycle of four steps, which is an approximation to the perfect heat engine. The cycle spans two isotherms, at two different temperatures, T_h and T_c, and two adiabats. In general a Carnot cycle involves four steps each of which are represented by the corresponding pressure-volume curves shown in Fig. 1.1. The first step is an isothermal expansion from volume V_1 to V_2. In this step the gas is placed in thermal contact with a heat source through any side of the container containing the gas, hence the gas expands and does work in pushing the piston. The second step is an adiabatic expansion, no heat exchange between the gas and the environment, from volume V_2 to V_3 which lowers the temperature of the gas from T_h to T_c. Still the gas does work in pushing the piston. The third step is another isothermal step, this time a compression, from V_3 to V_4. In this step the gas is placed in thermal contact with a heat sink. During this time the gas expels heat to the cold reservoir and work is done on the gas by the environment. The fourth and final step is an adiabatic compression to the original volume V_1 which raises the temperature from T_c to T_h due to the work done on the gas by the environment.

During this Carnot cycle, a quantity of heat H_1 is delivered to the gas at temperature T_h and a quantity of heat H_2 is rejected by the gas to the lower reservoir at temperature T_c, and the net work W is delivered to the outside. Work is done on/by the system at each of the four steps shown in Fig. 2.2. Hence the net work done for one carnot cycle

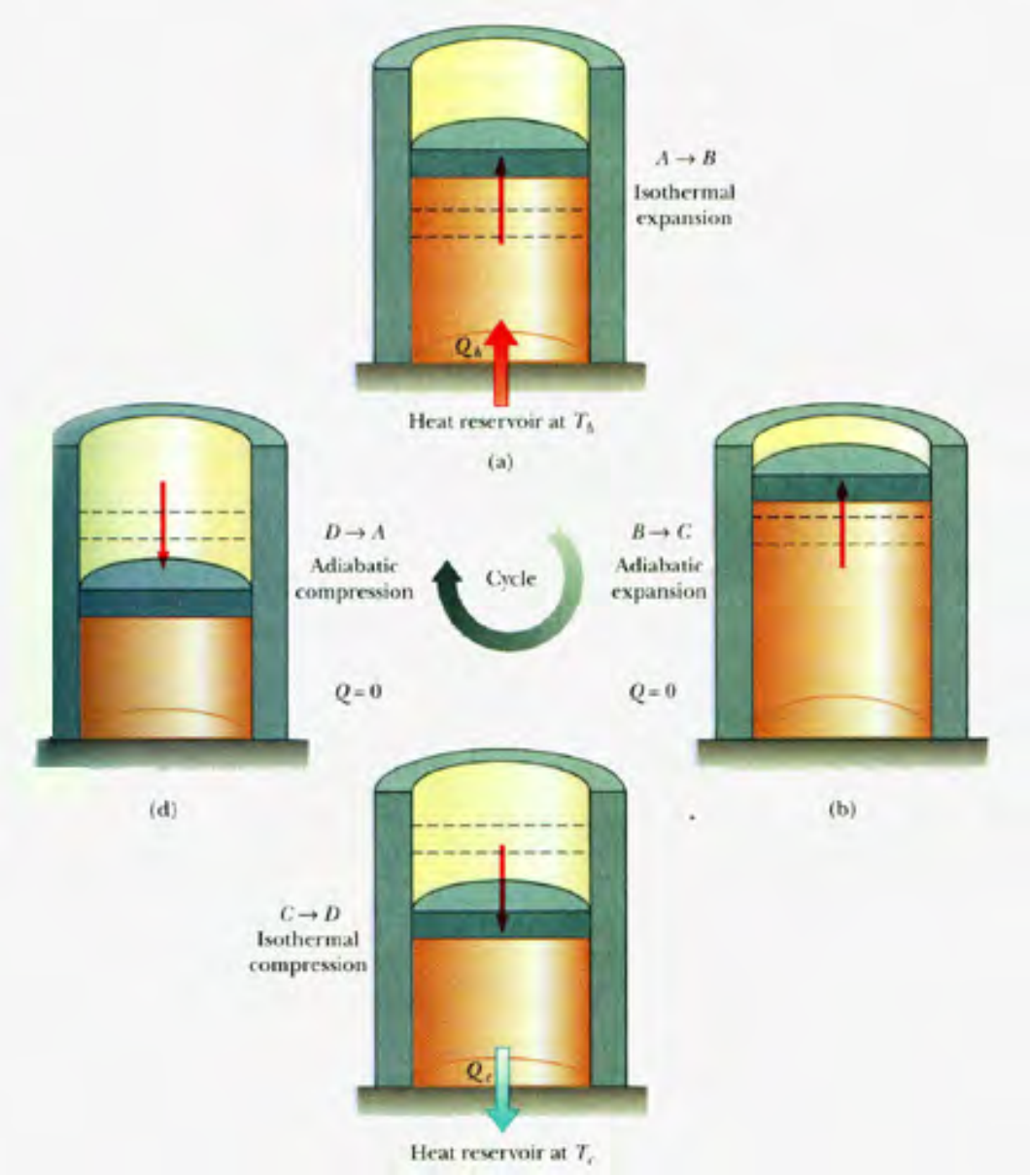

Figure 2.2: Carnot Cycle[40]

can be obtained from the sum of these works. In the first step, staying in contact with the hot reservior at temperature T_h, the gas expands isothermally from V_1 to V_2. During this process the work done by the gas is given by

$$W_{12} = \int_{V_1}^{V_2} PdV \tag{2.2.1}$$

Substituting for P from the equation of state for ideal gas, the work done in the first step can be rewritten as

$$W_{12} = \int_{V_1}^{V_2} \frac{NK_BT_h}{V} dV = NK_BT_h \ln \frac{V_2}{V_1} \tag{2.2.2}$$

where N is the number of gas molecules and K_B is Boltzmann constant. During isothermal process internal energy of an ideal gas remain unchanged, hence work done during the process equals the heat absorbed in the process.

$$H_1 = W_{12} = NK_BT_h \ln \frac{V_2}{V_1} \tag{2.2.3}$$

In the second step the gas expands adiabatically from V_2 to V_3 during which the temperature of the gas decreases from T_h to T_C. The work done in this process is given by

$$W_{23} = \int_{V_2}^{V_3} PdV \tag{2.2.4}$$

For adiabatic process we have

$$PV^\gamma = constant \tag{2.2.5}$$

$$\Longrightarrow P_2V_2^\gamma = P_3V_3^\gamma \tag{2.2.6}$$

Thus substituting for P in the equation for W_{23} yeilds

$$W_{23} = \int_{V_2}^{V_3} \frac{P_2V_2^\gamma}{V^\gamma} dV = \frac{P_3V_3 - P_2V_2}{1-\gamma} \tag{2.2.7}$$

Using the equation of state of an ideal gas one can write

$$\begin{aligned} P_2V_2 &= NK_BT_h \\ P_3V_3 &= NK_BT_C \\ P_3V_3 - P_2V_2 &= NK_B(T_C - T_h) \end{aligned} \tag{2.2.8}$$

Thus the equation for W_{23} can further be simplified to

$$W_{23} = \frac{NK_B(T_C - T_h)}{1-\gamma} = \frac{NK_B(T_h - T_C)}{\gamma - 1} \tag{2.2.9}$$

In the third step, staying in contact with the cold reservior at temperature T_C, the gas compresed isothermally from V_3 to V_4. During this process the work done on the gas is given by

$$W_{34} = \int_{V_3}^{V_4} PdV \tag{2.2.10}$$

Substituting for P from the equation of state for ideal gas, the work done in the third step can be rewritten as

$$W_{34} = \int_{V_3}^{V_4} \frac{NK_BT_C}{V} dV = NK_BT_C \ln \frac{V_4}{V_3} \tag{2.2.11}$$

where N is the number of gas molecules and K_B is Boltzmann constant. During isothermal process internal energy of an ideal gas remain unchanged, hence work done during the process equals the heat released in the process.

$$H_2 = -W_{34} = -NK_BT_C \ln \frac{V_4}{V_3} \tag{2.2.12}$$

In the fourth step, the last step of the cycle, the gas compressed adiabatically from V_4 to V_1. With similar approach to the second step, one can calculate the work done for this step and it becomes

$$W_{41} = \frac{NK_B(T_C - T_h)}{\gamma - 1} \tag{2.2.13}$$

The total work done in a reversible Carnot cycle is then

$$W = W_{12} + W_{23} + W_{34} + W_{41} = H_1 - H_2 = NK_B(T_h \ln \frac{V_2}{V_1} - T_C \ln \frac{V_3}{V_4}) \tag{2.2.14}$$

The thermal efficiency is then

$$\eta = \frac{W}{H_1} = 1 - \frac{NK_BT_C \ln \frac{V_3}{V_4}}{NK_BT_h \ln \frac{V_2}{V_1}} \tag{2.2.15}$$

From the relations; for isothermal process

$$PV = NK_BT = constant \tag{2.2.16}$$

and for adiabatic process

$$PV^{\gamma} = constant \tag{2.2.17}$$

we can obtain the relation

$$\frac{V_3}{V_4} = \frac{V_2}{V_1}. \tag{2.2.18}$$

Thus the thermal efficiency of a Carnot cycle, called Carnot efficiency, which is the upper limit for efficiency of any heat engine becomes

$$\eta_c = 1 - \frac{T_c}{T_h}. \tag{2.2.19}$$

All real engines are less efficient than the Carnot engine because they do not operate through a reversible cycle. The efficiency of a real engine is further reduced by different practical difficulties like friction, energy losses by conduction, etc.

2.3 Finite Time Thermodynamics

Traditional thermodynamics is a theory about equilibrium states and about limits on process variables for transformations from one equilibrium state to another. This traditional thermodynamics is extended to finite time thermodynamics (FTT) to obtain more realistic limits to the performance of real processes and hence FTT deals with processes which have explicit time or rate dependencies [9, 10].

The main role of classical thermodynamics in thermal engine analysis is providing upper bounds for process variables such as efficiency, work, heat and others. However, its bounds are usually far away from typical real values. Process of changing the state of a system while producing a minimum entropy or a minimum loss of availability, reversible process, need infinitely long process time. It is common, in many applications, to introduce a constraint for the available process time and this approach is known as finite time thermodynamics. FTT is usually known as a non-equilibrium theory. Its aim is to provide performance bounds and extremes for irreversible thermodynamic processes. Maximum power processes are at the center of interest of FTT. FTT provides an approach to quantify

cycles and plant components irreversibilities and thereafter can provide more applicable results for engineering design guidance.

Thermodynamics is believed to be started in 1826 when Sadi Carnot, French engineer, published his famous article "On The Motive Power Of Heat" [1]. The work is based on the formulation of bounds and optima for thermodynamic processes. Carnot showed that any engine which produces work taking heat from a heat reservior at temperature T_h has to deposit part of that heat in a colder reservior at T_c and the engine can have maximum efficiency called Carnot efficiency η_c. Non equilibrium thermodynamic theories developed as a result of science reality gap, i.e., Carnot efficiency can not be achieved in reality. FTT is one of these theories. One of the earliest concepts of FTT is the finite time potential.

Thermodynamics deals with energy conversion and the basic question of the area is how much work or heat can one get out of a system undergoing a thermodynamic process from one state to another? This question can be answered for certain reversible processes by the appropriate thermodynamic potentials. The potentials for reversible processes are characterized by the constancy of some state variables like T, P and V. Salamon and et. al. introduce extended potentials called finite time potentials which allow to handle a much wider class of constraints including those which depend on time; finite rate and finite time constraints [41]. Finite time potentials provide a bound for process variables in the form of the difference of their value between final and initial states. These bounds contain the losses by the irreversibilities and are thus more realistic than those for ordinary potentials. Eventhough FTT is a theory of irreversible processes, the systems are still described by equilibrium variables like P or T. This is because of a time scale separation, i.e., even though a system is not in equilibrium, parts of it can be considered to be very close to equilibrium because their internal relaxation time is much smaller than that of the total system. Thus the subsystem can be described very well by equilibrium terms. Thus a non equilibrium system can be considered as a collection of near equilibrium subsystems

which interact in an irreversible manner. Thermodynamic system is considered to consist of a number of equilibrium subsystems which interact in a highly irreversible way.

An extension of classical equilibrium thermodynamics to a thermal engine whose operation involve time dependent interaction process of the working substance of the engine with the surrounding while excluding possible irrevesibilities within the working substance is called endoreversible finite time thermodynamics (EFTT). The classical equilibrium thermodynamics can be extended to include irreversibility, production of entropy, caused by the transport to/from the system, otherwise the system internally is reversible. A typical endoreverible system is Curzon-Ahlborn engine, a Carnot type cycle in which there is no thermal equilibrium between the working fluid and the reservior and there exists a finite time heat transfer given by Newton's heat transfer law. Endoreversibility, excluding possible irreversibilities within the working substance, can be considered for cases in which the internal relaxation time of the working substance is negligibly short as compared to the total time of the cycle [11].

2.4 Efficiency at Maximum Power

2.4.1 Heat Engine With heat Losses Only

In 1975, Curzon and Ahlborn [3] considered the influence of finite rate heat transfer between the external heat reservoirs and the working fluid on the performance of a Carnot heat engine and obtained the eficiency of a Carnot engine at maximum power output. They could calculate the efficiency at maximum power by incorporating the effect of finite rate heat transfer between the working substance and the reserviors on Carnot engine. In order to have a cyclic process of transformation of heat energy in to work by a Carnot-like engine with in a finite time, the heat exchange between the working substance and the resorviors shoudn't be quasi-static. Rather there should be a temperature gradient, and hence the temperature T_1 of the working substance must be less than that of the hot

reservior T_h when it receives heat, $T_1 < T_h$, while its temperature T_2 must be greater than the temperature T_c of the cold reservior when it rejects heat, $T_c < T_2$. The larger the temperature gradient, the faster the heat is transmitted, the shorter the duration of a full cycle, and the less work W done in one cycle. The average power P of the engine is given by $P = W/\tau$, where τ is the period of the cycle. In the range between the maximum work done at infinite period with $P = 0$ and the vanishing work done for the shortest possible period with $P = 0$, there exists a temperature gradient at which the power output assumes a maximum value, and hence the efficiency of the engine at this particular point is called efficiency at maximum power. In calculating the efficiency at maximum power for an endoreverible Carnot-like engine, Curzon and Ahlborn consider finite rate heat transfer as the only possible source of irreversibility. It is assumed that the heat transfer between the reserviors and the working substance is governed by Newton's heat transfer law, linear dependence of heat flux on the temperature difference between the working substance and the reserviors. Let the amount of heat transfered from the hot reservior at T_H to the working substance at T_1 is

$$H_1 = \alpha t_1 (T_h - T_1) \tag{2.4.1}$$

where t_1 is time for the heat transfer and α is proportionality constant. Similarly heat transfered from the working substance at T_2 to the cold reservior at T_C is

$$H_2 = \beta t_2 (T_2 - T_c) \tag{2.4.2}$$

Applying isentropic property for the endoreversible process yields

$$\frac{H_1}{T_1} = \frac{H_2}{T_2} \tag{2.4.3}$$

The work done by the engine is given by

$$W = H_1 - H_2 \tag{2.4.4}$$

The power output by the engine is then

$$P = \frac{W}{\tau} = \frac{H_1 - H_2}{\tau} \tag{2.4.5}$$

where τ is the total cycle time or period of the cyclic process. Assuming instatntaneous adiabatic process, the period of the cyclic process can be approximated to be

$$\tau \approxeq t_1 + t_2 \tag{2.4.6}$$

Let $T_h = T_1 + x$ and $T_c = T_2 - y$. Thus eqn (2.4.3) can be rewritten as

$$\frac{H_1}{T_h - x} = \frac{H_2}{T_c + y} \tag{2.4.7}$$

$$H_1 = \frac{T_h - x}{T_c + y} H_2 \tag{2.4.8}$$

$$\begin{aligned} H_1 - H_2 &= \frac{T_h - x}{T_c + y} H_2 - H_2 \\ &= (\frac{T_h - x}{T_c + y} - 1) H_2 \\ &= \frac{T_h - T_c - x - y}{T_c + y} H_2 \end{aligned} \tag{2.4.9}$$

Similarly from eqns (2.4.1) and (2.4.2) we can write

$$\begin{aligned} t_1 &= \frac{H_1}{\alpha x} \\ t_2 &= \frac{H_2}{\beta y} \end{aligned} \tag{2.4.10}$$

$$\begin{aligned} t_1 + t_2 &= \frac{H_1}{\alpha x} + \frac{H_2}{\beta y} \\ &= \frac{\beta y H_1 + \alpha x H_2}{\alpha \beta x y} \\ &= \frac{\beta y \frac{T_h - x}{T_c + y} H_2 + \alpha x H_2}{\alpha \beta x y} \\ &= \frac{\beta y (T_h - x) + \alpha x (T_c + y)}{\alpha \beta x y (T_c + y)} H_2 \end{aligned} \tag{2.4.11}$$

Substituting eqns (2.4.6), (2.4.9) and (2.4.11) in eqn (2.4.5) yields

$$\begin{aligned} P &= \frac{H_1 - H_2}{t_1 + t_2} \\ &= \frac{(T_h - T_c - x - y) H_2}{T_c + y} \frac{\alpha \beta x y (T_c + y)}{(\beta y (T_h - x) + \alpha x (T_c + y)) H_2} \\ &= \frac{\alpha \beta x y (T_h - T_c - x - y)}{\beta T_h y + \alpha T_c x + x y (\alpha - \beta)} \end{aligned} \tag{2.4.12}$$

The first derivative of power P with respect to x is then

$$\frac{\partial P}{\partial x} = \frac{\alpha\beta y(T_h - T_c - 2x - y)(\beta T_h y + \alpha T_c x + xy(\alpha - \beta)) - (\alpha T_c + y(\alpha - \beta))\alpha\beta xy(T_h - T_c - x - y)}{(\beta T_h y + \alpha T_c x + xy(\alpha - \beta))^2} \tag{2.4.13}$$

But at maximum value $P = P_{max}$ it should vanish, $\frac{\partial P}{\partial x} \mid_{P=P_{max}} = \frac{\partial P}{\partial y} \mid_{P=P_{max}} = 0$. Hence it follows

$$\begin{aligned}
\alpha\beta y(T_h - T_c - 2x - y)(\beta T_h y + \alpha T_c x + xy(\alpha - \beta)) &= \alpha\beta xy(T_h - T_c - x - y)(\alpha T_c + y(\alpha - \beta)) \\
(T_h - T_c - 2x - y)(\beta T_h y + \alpha T_c x + xy(\alpha - \beta)) &= (T_h - T_c - x - y)(\alpha T_c x + xy(\alpha - \beta)) \\
(T_h - T_c - 2x - y)\beta T_h y &= (\alpha T_c x + xy(\alpha - \beta)) \\
&* \ ((T_h - T_c - x - y) - (T_h - T_c - 2x - y)) \\
(T_h - T_c - x - y)\beta T_h y &= (\alpha T_c x + xy(\alpha - \beta))x \\
\beta T_h y(T_h - T_c - 2x - y) &= x(\beta T_h y + \alpha T_c x + xy(\alpha - \beta))
\end{aligned} \tag{2.4.14}$$

Similarly

$$\frac{\partial P}{\partial y} = \frac{\alpha\beta x(T_h - T_c - x - 2y)(\beta T_h y + \alpha T_c x + xy(\alpha - \beta)) - (\beta T_h + x(\alpha - \beta))\alpha\beta xy(T_h - T_c - x - y)}{(\beta T_h y + \alpha T_c x + xy(\alpha - \beta))^2} \tag{2.4.15}$$

$$\begin{aligned}
\alpha\beta x(T_h - T_c - x - 2y)(\beta T_h y + \alpha T_c x + xy(\alpha - \beta)) &= \alpha\beta xy(T_h - T_c - x - y)(\beta T_h + x(\alpha - \beta)) \\
(T_h - T_c - x - 2y)\alpha T_c x &= y(\beta T_h + x(\alpha - \beta)) \\
&* \ ((T_h - T_c - x - y) - (T_h - T_c - x - 2y)) \\
\alpha T_c x(T_h - T_c - x - y) - \alpha T_c xy &= y(\beta T_h y + xy(\alpha - \beta)) \\
\alpha T_c x(T_h - T_c - x - y) &= y(\beta T_h y + \alpha T_c x + xy(\alpha - \beta))
\end{aligned} \tag{2.4.16}$$

Dividing eqn (2.4.14) by (2.4.16) yields

$$\begin{aligned}
\frac{\beta T_h y}{\alpha T_c x} &= \frac{x}{y} \\
\beta T_h y^2 &= \alpha T_c x^2 \\
y &= \sqrt{\frac{\alpha T_c}{\beta T_h}} x
\end{aligned} \tag{2.4.17}$$

Substituting eqn (2.4.17) in (2.4.16) yields the following quadratic equation

$$Ax^2 + Bx + C = 0 \tag{2.4.18}$$

Where; $A = \frac{\alpha T_c}{\beta T_h}(\alpha - \beta)$, $B = 2\alpha T_c(\sqrt{\frac{\alpha T_c}{\beta T_h}} + 1)$ and $C = \alpha T_c(T_c - 1)$. Equation (2.4.18) can be rewritten as

$$x^2 + bx + c = 0 \tag{2.4.19}$$

where $b = \frac{2\beta T_h}{\alpha - \beta}(\sqrt{\frac{\alpha T_c}{\beta T_h}} + 1)$ and $c = \frac{\beta T_1}{\alpha - \beta}(T_c - T_h)$ The solution for this equation is then

$$x = \frac{1}{2}[-\frac{2\beta T_c}{\alpha - \beta}(\sqrt{\frac{\alpha T_c}{\beta T_h}} + 1) \pm \sqrt{\frac{4(\beta T_c)^2}{(\alpha - \beta)^2} - \frac{4\beta T_c}{\alpha - \beta}(T_c - T_h)}] \tag{2.4.20}$$

$$x = T_h[-\frac{1}{\frac{\alpha}{\beta} - 1}(\sqrt{\frac{\alpha T_c}{\beta T_h}} + 1) \pm \sqrt{(\frac{1}{\frac{\alpha}{\beta} - 1})^2(\sqrt{\frac{\alpha T_c}{\beta T_h}} + 1)^2 - \frac{1}{\frac{\alpha}{\beta} - 1}(\frac{T_c}{T_h} - 1)}] \tag{2.4.21}$$

$$x = T_h\frac{-(1 + \sqrt{\frac{\alpha T_c}{\beta T_h}}) \pm \sqrt{1 + \frac{\alpha T_c}{\beta T_h} + 2\sqrt{\frac{\alpha T_c}{\beta T_h}} - (\sqrt{\frac{T_c}{T_h}} - 1)(\sqrt{\frac{T_c}{T_h}} + 1)(\sqrt{\frac{\alpha}{\beta}} - 1)(\sqrt{\frac{\alpha}{\beta}} + 1)}}{(\sqrt{\frac{\alpha}{\beta}} - 1)(\sqrt{\frac{\alpha}{\beta}} + 1)} \tag{2.4.22}$$

$$\sqrt{1 + \frac{\alpha T_c}{\beta T_h} + 2\sqrt{\frac{\alpha T_c}{\beta T_h}} - (\sqrt{\frac{T_c}{T_h}} - 1)(\sqrt{\frac{T_c}{T_h}} + 1)(\sqrt{\frac{\alpha}{\beta}} - 1)(\sqrt{\frac{\alpha}{\beta}} + 1)} = \sqrt{1 + \frac{\alpha T_c}{\beta T_h} + 2\sqrt{\frac{\alpha T_c}{\beta T_h}} - (a - b)(a + b)} \tag{2.4.23}$$

where $a = \sqrt{\frac{\alpha T_c}{\beta T_h}} + 1$ and $b = \sqrt{\frac{\alpha}{\beta}} + \sqrt{\frac{T_c}{T_h}}$

$$(a - b)(a + b) = (a^2 - b^2) = \frac{\alpha T_c}{\beta T_h} + 1 - \frac{\alpha}{\beta} - \frac{T_c}{T_h} \tag{2.4.24}$$

Thus we can have

$$\sqrt{1 + \frac{\alpha T_c}{\beta T_h} + 2\sqrt{\frac{\alpha T_c}{\beta T_h}} - (\sqrt{\frac{T_c}{T_h}} - 1)(\sqrt{\frac{T_c}{T_h}} + 1)(\sqrt{\frac{\alpha}{\beta}} - 1)(\sqrt{\frac{\alpha}{\beta}} + 1)} = \sqrt{\frac{\alpha}{\beta}} + \sqrt{\frac{T_c}{T_h}} \tag{2.4.25}$$

$$\Rightarrow x = T_h\frac{-(1 + \sqrt{\frac{\alpha T_c}{\beta T_h}}) \pm (\sqrt{\frac{\alpha}{\beta}} + \sqrt{\frac{T_c}{T_h}})}{(\sqrt{\frac{\alpha}{\beta}} - 1)(\sqrt{\frac{\alpha}{\beta}} + 1)} \tag{2.4.26}$$

$$\Rightarrow x_1 = T_h \frac{-(1+\sqrt{\frac{\alpha T_c}{\beta T_h}}) + (\sqrt{\frac{\alpha}{\beta}} + \sqrt{\frac{T_c}{T_h}})}{(\sqrt{\frac{\alpha}{\beta}} - 1)(\sqrt{\frac{\alpha}{\beta}} + 1)} = T_h \frac{1 - \sqrt{\frac{T_c}{T_h}}}{1 + \sqrt{\frac{\alpha}{\beta}}} \tag{2.4.27}$$

$$\Rightarrow x_2 = T_h \frac{-(1+\sqrt{\frac{\alpha T_c}{\beta T_h}}) - (\sqrt{\frac{\alpha}{\beta}} - \sqrt{\frac{T_c}{T_h}})}{(\sqrt{\frac{\alpha}{\beta}} - 1)(\sqrt{\frac{\alpha}{\beta}} + 1)} = T_h \frac{1 + \sqrt{\frac{T_c}{T_h}}}{1 - \sqrt{\frac{\alpha}{\beta}}} \tag{2.4.28}$$

$$\frac{1 + \sqrt{\frac{T_c}{T_h}}}{1 - \sqrt{\frac{\alpha}{\beta}}} > 1$$
$$\Rightarrow x_2 > T_h \tag{2.4.29}$$

But we have $T_1 = T_h - x$ and T_1 must be greater than zero. Hence x_2 is non-physical root. Thus the real root is x_1

$$x = x_1 = T_h \frac{1 - \sqrt{\frac{T_c}{T_h}}}{1 + \sqrt{\frac{\alpha}{\beta}}} \tag{2.4.30}$$

Then y becomes

$$y = \sqrt{\frac{\alpha T_c}{\beta T_h}} x = \sqrt{\frac{\alpha T_c}{\beta T_h}} T_h \frac{1 - \sqrt{\frac{T_c}{T_h}}}{1 + \sqrt{\frac{\alpha}{\beta}}} \tag{2.4.31}$$

$$y = T_h \frac{\frac{T_c}{T_h}(\frac{T_h}{T_c}\sqrt{\frac{T_c}{T_h}} - 1)}{\sqrt{\frac{\alpha}{\beta}}(1 + \sqrt{\frac{\alpha}{\beta}})} = T_c(\frac{\sqrt{\frac{T_h}{T_c}} - 1}{\sqrt{\frac{\beta}{\alpha}} + 1}) \tag{2.4.32}$$

Efficiency for an endoreversible heat engine is then given by

$$\eta = 1 - \frac{H_2}{H_1} = 1 - \frac{T_2}{T_1} = 1 - \frac{T_c + y}{T_h - x} \tag{2.4.33}$$

$$\frac{T_c + y}{T_h - x} = \frac{T_c + \frac{T_c(\sqrt{\frac{T_h}{T_c}} - 1)}{\sqrt{\frac{\beta}{\alpha}} + 1}}{T_h - \frac{T_h(1 - \sqrt{\frac{T_c}{T_h}})}{1 + \sqrt{\frac{\alpha}{\beta}}}} = \frac{T_c}{T_h}(\frac{\sqrt{\frac{\beta}{\alpha}} + 1 + \sqrt{\frac{T_h}{T_c}} - 1}{\sqrt{\frac{\alpha}{\beta}} + 1 + \sqrt{\frac{T_c}{T_h}} - 1})\frac{\sqrt{\frac{\alpha}{\beta}} + 1}{\sqrt{\frac{\beta}{\alpha}} + 1} \tag{2.4.34}$$

$$\frac{T_c + y}{T_h - x} = \frac{T_c}{T_h} \frac{\sqrt{\frac{T_h}{T_c}}(\sqrt{\frac{\beta}{\alpha}}\sqrt{\frac{T_c}{T_h}} + \sqrt{\frac{T_c}{T_h}} + 1 + \sqrt{\frac{\alpha}{\beta}})}{\sqrt{\frac{\beta}{\alpha}}\sqrt{\frac{T_c}{T_h}} + \sqrt{\frac{T_c}{T_h}} + 1 + \sqrt{\frac{\alpha}{\beta}}} = \sqrt{\frac{T_c}{T_h}} \tag{2.4.35}$$

Thus efficiency at maximum power becomes

$$\eta_{CA} = 1 - \sqrt{\frac{T_c}{T_h}}. \tag{2.4.36}$$

In this case the only source of irreversibility in the engine is a linear finite rate heat transfer between the working fluid and its two heat reservoirs. And hence, the process is called endoreversible.

2.4.2 Heat Engine With Friction Losses Only

It is acknowledged that the Curzon-Ahlborn efficiency η_{CA} determines the efficiency at maximum power of a heat engine which only affected by the irreversibility of finite rate heat transfer (endoreversible engines). This is conceptually different from the role of the Carnot efficiency η_C which is indeed the upper bound of the efficiencies of all heat engines. Although the efficiencies of real heat engines can not attain the Carnot efficiency, it is possible, and often desirable, for their efficiencies to be larger than their respective maximum power efficiencies. In fact, the maximum power efficiency is the allowable lower bound of the efficiency for a given class of heat engines [16]. In reference [17], M. Esposito et.al. cleared that CA efficiency is an exact property of Carnot machines operating at low, symmetric dissipation. They have also put upper and lower boundary for the efficiency of Carnot machines operating at low, asymmetric dissipation. Though it is not an upper or lower bound, CA-efficiency describes the efficiency of actual power plants to a good approximation [3,11]. Beside the finite rate heat transfer that considered in the Curzon-Ahlborn engine there are other possible sources of irreversibilities which affect efficiency of heat engine. Different laws of heat transfer also have significant effect on the efficiency performance limit of the irreversible heat engines [34,35, 36]. In this section, however, we would like to discuss the impact of heat losses on the prformance efficiency of heat engine.

Consider a Carnot-like heat engine for which there is no temperature gradients, and hence no heat losses but friction losses. Suppose there is a friction between the piston and the wall of the cylinder containing the working substance, hence during the motion of the

piston work is lost due to friction. In this case we are dealing with a Carnot-like cycle with friction losses only. The influence of friction is similar to that of heat conduction. For infinite period the friction losses are negligibly small, but $P = 0$. With increasing speed of the process and simultaneously decreasing efficiency, the friction losses become larger until they eat up the entire work done such that again $P = 0$. In between, there is a process rate at which the power output becomes maximal while the efficiency is below its maximum [14]. The total force acting on the piston can be formulated as

$$F = PA - \mu v(t) \tag{2.4.37}$$

where P is pressure on the piston, A is surface area of the piston, μ is coefficient of friction, $v(t) = \dot{x}$ is speed of the piston and x is displacement of the piston. The work done by the piston which moves a displacement dx is

$$\begin{aligned} dW &= Fdx \\ &= (PA - \mu v(t))dx \\ &= (PA - \mu \dot{x})dx \\ &= PAdx - \mu \frac{\partial x}{\partial t}\frac{\partial x}{\partial t}dt \\ &= Pdv - \mu v^2(t)dt \end{aligned} \tag{2.4.38}$$

The workdone for a complete cycle is then

$$W = \oint PdV - \mu \oint v^2(t)dt \tag{2.4.39}$$

It is known, from first law of thermodynamics, that change in internal energy of a system for a complete cycle is zero.

$$\oint du = \oint \delta H - \oint PdV = 0 \tag{2.4.40}$$

$$\oint PdV = \oint \delta H = H_1 - H_2 \tag{2.4.41}$$

$$W = H_1 - H_2 - \mu \oint v^2(t)dt \tag{2.4.42}$$

Suppose $v(t)$ is self-similar, such that

$$v(t) = v^* g(\frac{t}{\tau}) \tag{2.4.43}$$

where $g(\frac{t}{\tau})$ is a periodic function of $\frac{t}{\tau}$ with period 1, v^* is a measure of the speed of the process. The distance covered by the piston during a complete cycle is

$$\begin{aligned} 2D &= \oint \mid v(t) \mid dt \\ &= v^* \oint \mid g(\frac{t}{\tau}) \mid dt \end{aligned} \tag{2.4.44}$$

The time average of the periodic function $\mid g(\frac{t}{\tau}) \mid$ over one cycle of period τ is

$$\overline{g(\frac{t}{\tau})} = \frac{1}{\tau}\int_0^\tau g(\frac{t}{\tau})dt \tag{2.4.45}$$

$$2D = v^*\tau\overline{g(\frac{t}{\tau})} \tag{2.4.46}$$

$$v^* = \frac{2D}{\tau\overline{g(\frac{t}{\tau})}} \tag{2.4.47}$$

$$\begin{aligned} \oint v^2(t)dt &= v^{*2}\oint g^2(\frac{t}{\tau})dt \\ &= v^{*2}\tau\overline{g^2(\frac{t}{\tau})} \\ &= \frac{4D^2}{(\overline{\mid g(\frac{t}{\tau}) \mid})^2}\frac{\tau\overline{g^2(\frac{t}{\tau})}}{\tau^2} \\ &= \frac{\overline{g^2(\frac{t}{\tau})}}{(\overline{\mid g(\frac{t}{\tau}) \mid})^2}\frac{4D^2}{\tau} \\ &= \delta\frac{4D^2}{\tau} \end{aligned} \tag{2.4.48}$$

where $\delta = \frac{\overline{g^2(\frac{t}{\tau})}}{(\overline{|g(\frac{t}{\tau})|})^2}$ is a fixed parameter for a Carnot-like engine.

$$W = H_1 - H_2 - \mu\delta\frac{4D^2}{\tau} \tag{2.4.49}$$

The power of the engine is then

$$P = \frac{W}{\tau} = \frac{H_1 - H_2}{\tau} - \mu\delta\frac{4D^2}{\tau^2} \tag{2.4.50}$$

While the efficiency is

$$\eta = \frac{W}{H_1} = \frac{H_1 - H_2}{H_1} - \mu\delta\frac{4D^2}{\tau H_1} \tag{2.4.51}$$

Between the shortest possible cycle period and infinite cycle period, $\tau = \infty$, the power P has a maximum value corresponding to τ_{max}, a cycle period at maximum power, which can be determined from

$$\frac{dP(\tau)}{d\tau} \mid_{\tau=\tau_{max}} = 0 \tag{2.4.52}$$

$$\tau_{max} = \frac{8\mu\delta D^2}{H_1 - H_2} \tag{2.4.53}$$

The efficiency at maximum power of a Carnot-like heat engine with friction loses only is then obtained by substituting eqn (2.4.53) for τ in (2.4.51) and becomes

$$\begin{aligned} \eta_{max} &= \frac{H_1 - H_2}{H_1} - \mu\delta\frac{4D^2}{\tau_{max} H_1} \\ &= \frac{H_1 - H_2}{H_1} - \mu\delta\frac{4D^2}{H_1}\frac{H_1 - H_2}{8\mu\delta D^2} \\ &= \frac{1}{2}(1 - \frac{H_2}{H_1}) \\ &= \frac{1}{2}\eta_c \end{aligned} \tag{2.4.54}$$

This implies that any loss in energy due to friction in heat engine reduce the efficieny at maximum power of the engine to half of the Carnot efficiency.

2.4.3 Heat Engine With both Friction And Heat Losses

For a Carnot-like heat engine with heat losses only efficiency of the engine is given by eqn (2.4.33) and the period of the process is, from eqn (2.4.6)

$$\begin{aligned}
\tau = t_1 + t_2 &= \frac{\alpha x H_2 + \beta y H_1}{\alpha\beta xy} \\
&= \frac{\alpha x \frac{T_c+y}{T_h-x} H_1 + \beta y H_1}{\alpha\beta xy} \\
&= \frac{\frac{\alpha x H_1}{(T_h-x)(T_h-x)} + \frac{\beta y H_1}{(T_c+y)(T_h-x)}}{\alpha\beta \frac{x}{T_h-x}\frac{y}{T_c+y}} \\
&= \frac{H_1}{T_h-x}[\frac{\frac{\alpha x}{(T_h-x)} + \frac{\beta y}{(T_c+y)}}{\alpha\beta \frac{x}{T_h-x}\frac{y}{T_c+y}}] \\
&= \frac{H_1}{T_h-x}[\frac{1}{\frac{\beta y}{T_c+y}} + \frac{1}{\frac{\alpha x}{T_h-x}}] \\
&= \frac{H_1}{T_h-x}[\frac{T_c+y}{\beta y} + \frac{T_h-x}{\alpha x}] \\
&= \frac{H_1}{\beta(T_h-x)}[\frac{T_c+y}{y} + \frac{\beta(T_h-x)}{\alpha x}] \\
&= \frac{H_1}{\beta}[\frac{T_c+y}{y(T_h-x)} + \frac{\beta}{\alpha x}] \\
&= \frac{H_1}{\beta}[\frac{T_c+y}{y(T_h-x)} + \frac{\mu}{\alpha}] \\
&= \frac{H_1}{\beta}[\frac{N}{xy(T_h-x)}] \qquad (2.4.55)
\end{aligned}$$

where $\mu = \frac{\beta}{\alpha}$ and $N = x(T_c + y) + \mu y(T_h - x)$.

For a Carnot-like engine with both friction and heat losses the period of the process is given by

$$\tau = \frac{H_1}{\beta}[\frac{N}{xy(T_h-x)}] \qquad (2.4.56)$$

while the efficiency of the engine is, by eqn (2.4.51)

$$\begin{aligned}
\eta &= \frac{W}{H_1} = \frac{H_1 - H_2}{H_1} - \mu\delta\frac{4D^2}{\tau H_1} \\
&= \frac{H_1 - H_2}{H_1} - \mu\delta\frac{4D^2}{H_1\frac{H_1}{\beta}[\frac{N}{xy(T_h-x)}]} \\
&= 1 - \frac{T_c+y}{T_h-x} - \mu\delta\frac{4D^2\beta xy(T_h-x)}{NH_1^2} \qquad (2.4.57)
\end{aligned}$$

The amount of heat transfered, H_1, from the heat source to the system in a process involving heat loss is, from eqn (2.2.3)

$$H_1 = R(T_h - x)\ln\frac{V_2}{V_1} \tag{2.4.58}$$

where we assume one mole system, $n = 1$. Then eqn (2.4.57) can be rewritten as

$$\begin{aligned}\eta &= 1 - \frac{T_c + y}{T_h - x} - \mu\delta\frac{4D^2\beta xy(T_h - x)}{NR^2(T_h - x)^2\ln^2\frac{V_2}{V_1}} \\ &= 1 - \frac{T_c + y}{T_h - x} - \frac{\lambda xy}{N(T_h - x)}\end{aligned} \tag{2.4.59}$$

where $\lambda = \frac{4\mu\delta\beta D^2}{R^2\ln^2\frac{V_2}{V_1}}$. The output power of the engine per cycle can be given by

$$\begin{aligned}P &= \frac{\eta H_1}{\tau} \\ &= \frac{H_1[1 - \frac{T_c+y}{T_h-x} - \frac{\lambda xy}{N(T_h-x)}]}{\frac{H_1}{\beta}[\frac{N}{xy(T_h-x)}]} \\ &= \frac{1}{N}[1 - \frac{T_c + y}{T_h - x} - \frac{\lambda xy}{N(T_h - x)}]\beta xy(T_h - x) \\ &= [\frac{(T_h - x - T_c - y)xy}{N} - \frac{\lambda x^2y^2}{N^2}]\beta\end{aligned} \tag{2.4.60}$$

Any adiabatic process by ideal gas satisfies

$$TV^{\gamma-1} = constant \tag{2.4.61}$$

Thus considering point 2 and point 3 in Fig. 1.1 we can write

$$\begin{aligned}T_2V_2^{\gamma-1} &= T_3V_3^{\gamma-1} \\ (T_h - x)V_2^{\gamma-1} &= (T_c + y)V_3^{\gamma-1} \\ (\frac{V_2}{V_3})^{\gamma-1} &= \frac{T_c + y}{T_h - x} \\ \frac{V_2}{V_1} &= \frac{V_3}{V_1}(\frac{T_c + y}{T_h - x})^{\frac{1}{\gamma-1}}\end{aligned} \tag{2.4.62}$$

Using $V_1 = AD_1$ and $V_3 = A(D_1 + D)$, we can have

$$\frac{V_3}{V_1} = 1 + d \tag{2.4.63}$$

where $d = \frac{D}{D_1}$, D_1 and $D_1 + D$ are the length of the box when the piston is at point 1 and point 3 respectively in Fig. 1.1. Thus eqn (2.4.62) becomes

$$\frac{V_2}{V_1} = (1+d)(\frac{T_c + y}{T_h - x})^{\frac{1}{\gamma-1}} \tag{2.4.64}$$

$$\begin{aligned}
\lambda &= \frac{4\mu\delta\beta D^2}{R^2 \ln^2 \frac{V_2}{V_1}} \\
&= \frac{4\mu\delta\beta D^2}{R^2 \ln^2[(1+d)(\frac{T_c+y}{T_h-x})^{\frac{1}{\gamma-1}}]} \\
&= \frac{4\mu\delta\beta D^2}{R^2 \ln^2[(1+d)(\rho\frac{1+\frac{y}{T_c}}{1-\frac{x}{T_h}})^{\frac{1}{\gamma-1}}]} \\
&= \frac{4\mu\delta\beta D^2}{R^2[\ln(1+d) + \frac{1}{\gamma-1}\ln\rho + \frac{1}{\gamma-1}\ln\frac{1+\frac{y}{T_C}}{1-\frac{x}{T_h}}]^2} \qquad (2.4.65) \\
&\approx \frac{4\mu\delta\beta D^2}{R^2[\ln(1+d) + \frac{1}{\gamma-1}\ln\rho]^2} \qquad (2.4.66)
\end{aligned}$$

Between very slow and very fast cycle speed, there must be a point of maximum power operation, which can be determined from the partial derivatives of P with respect to x and y and letting the result equal to zero. Using the following equations for N, $\frac{\partial N}{\partial x}$ and $\frac{\partial N}{\partial y}$

$$N = x(T_c + y) + \mu y(T_h - x) \tag{2.4.67}$$

$$\frac{\partial N}{\partial x} = T_c + y(1-\mu) \tag{2.4.68}$$

$$\frac{\partial N}{\partial y} = \mu T_h + x(1-\mu) \tag{2.4.69}$$

the partial derivatives of P with respect to x and y can be computed from eqn (2.4.60) and respectively given as

$$\frac{\partial P}{\partial x} = \frac{Ny(T_h - T_c - 2x - y) - xy(T_h - T_c - x - y)[T_c + y(1-\mu)]}{N^2} - \frac{2\lambda xy^2N^2 - 2N\lambda x^2y^2[T_c + y(1-\mu)]}{N^4} \tag{2.4.70}$$

$$\frac{\partial P}{\partial y} = \frac{Nx(T_h - T_c - x - 2y) - xy(T_h - T_c - x - y)[\mu T_h + x(1-\mu)]}{N^2} - \frac{2\lambda x^2yN^2 - 2N\lambda x^2y^2[\mu T_h + x(1-\mu)]}{N^4} \tag{2.4.71}$$

Setting the above equations to be equal to zero yeilds

$$N^2y(T_h - T_c - 2x - y) - Ny(T_h - T_c - x - y)(N - \mu yT_h) - 2N\lambda xy^2 + 2\lambda xy^2(N - \mu yT_h) = 0$$

$$N^2x(T_h - T_c - x - 2y) - Nx(T_h - T_c - x - y)(N - xT_c) - 2N\lambda x^2y + 2\lambda x^2y(N - xT_c) = 0$$

Which can be rewritten as

$$-N^2xy + \mu Ny^2T_h(T_h - T_c - x - y) - 2\lambda xy^3\mu T_h = 0 \tag{2.4.72}$$

$$-N^2xy + Nx^2T_c(T_h - T_c - x - y) - 2\lambda x^3yT_c = 0 \tag{2.4.73}$$

Multiplying eqn (2.4.72) by x^2T_c and eqn (2.4.73) by μy^2T_h and solving simultaneously yeilds

$$y = x\sqrt{\frac{\rho}{\mu}} \tag{2.4.74}$$

where $\rho = \frac{T_c}{T_h}$.

Substituting eqn (2.4.74) in eqn (2.4.67) yeilds

$$\begin{aligned} N &= x(T_c + x\sqrt{\frac{\rho}{\mu}}) + \mu x\sqrt{\frac{\rho}{\mu}}(T_h - x) \\ &= xT_c + x^2\sqrt{\frac{\rho}{\mu}} + \mu xT_h\sqrt{\frac{\rho}{\mu}} - \mu x^2\sqrt{\frac{\rho}{\mu}} \\ &= \sqrt{\frac{\rho}{\mu}}(xT_c\sqrt{\frac{\mu}{\rho}} + \mu xT_h + x^2(1-\mu)) \end{aligned} \tag{2.4.75}$$

With the help of eqns (2.4.74) and (2.4.75), eqn (2.4.73) can be rewritten as

$$-\frac{\rho}{\mu}[xT_c\sqrt{\frac{\mu}{\rho}}+\mu xT_h+x^2(1-\mu)]^2+T_c(T_h-T_c-x-x\sqrt{\frac{\rho}{\mu}})[xT_c\sqrt{\frac{\mu}{\rho}}+\mu xT_h+x^2(1-\mu)]-2\lambda x^2T_c = 0 \tag{2.4.76}$$

For $\mu = 1$ we can have

$$-\rho x^2[T_c\sqrt{\frac{1}{\rho}} + T_h]^2 + xT_c(T_h - T_c - x - x\sqrt{\rho})[T_c\sqrt{\frac{1}{\rho}} + T_h] - 2\lambda x^2T_c = 0 \tag{2.4.77}$$

which can be rearranged to

$$x[\rho[T_c\sqrt{\frac{1}{\rho}} + T_h]^2 + T_c(1 + \sqrt{\rho})[T_c\sqrt{\frac{1}{\rho}} + T_h] + 2\lambda T_c] = T_c(T_h - T_c)[T_c\sqrt{\frac{1}{\rho}} + T_h] \tag{2.4.78}$$

Then solving for x yeilds

$$x = \frac{T_h(1-\sqrt{\rho})}{2(1+\frac{\lambda}{T_h(1+\sqrt{\rho})^2})} \tag{2.4.79}$$

For $\mu = 1$ eqn (2.4.75) becomes

$$N = xT_h\sqrt{\rho}(1+\sqrt{\rho}) \tag{2.4.80}$$

The efficiency of the Carnot-like engine with both heat and friction losses, eqn (2.4.59), becomes

$$\begin{aligned}
\eta_{max} &= 1 - \frac{T_c + y}{T_h - x} - \frac{\lambda xy}{N(T_h - x)} \\
&= 1 - \frac{T_c + x\sqrt{\rho}}{T_h - x} - \frac{\lambda x^2\sqrt{\rho}}{xT_h\sqrt{\rho}(1+\sqrt{\rho})(T_h - x)} \\
&= 1 - \frac{T_c + x\sqrt{\rho}}{T_h - x} - \frac{\lambda x}{T_h(1+\sqrt{\rho})(T_h - x)} \\
&= \frac{T_h(1+\sqrt{\rho})(T_h - x) - T_h(1+\sqrt{\rho})(T_c + x\sqrt{\rho}) - \lambda x}{T_h(1+\sqrt{\rho})(T_h - x)} \\
&= \frac{T_h(1-\rho) - x(1+\sqrt{\rho}) - \frac{\lambda x}{T_h(1+\sqrt{\rho})}}{T_h - x} \\
&= \frac{T_h(1-\sqrt{\rho}) - x(1+\frac{\lambda}{T_h(1+\sqrt{\rho})^2})}{T_h - x}(1+\sqrt{\rho})
\end{aligned} \tag{2.4.81}$$

Substituting eqn (2.4.79) in (2.4.81) and after some rearrangement one can obtain

$$\eta_{max} = \frac{1+\frac{\lambda}{T_h(1+\sqrt{\rho})^2}}{1+\frac{2\lambda}{T_h(1+\sqrt{\rho})^3}}(1-\sqrt{\rho}) \tag{2.4.82}$$

If friction loss is negligible, $\lambda \approxeq 0$, eqn (2.4.82) reduces to the familiar Curzon-Ahlborn efficiency

$$\eta_{max} = 1 - \sqrt{\rho} = \eta_{CA} \tag{2.4.83}$$

Where as when friction dominates, $\lambda \gg 1$, eqn (2.4.82) reduces to eqn (2.4.54) as it should.

2.5 Optimization between Efficiency and Power

It is well known that transport is almost totally dependent on fossil fuels, particularly, petroleum-based fuels such as gasoline, diesel fuel and natural gas. As a consequence

fuel consumption and emission by the transport sector, and hence performance efficiency of a heat engine, become important issues of these days. Any heat engine working at maximum power leads to substancial amount of the input energy to be wasted. On the contrary, working at maximum efficiency has no practical importance. Hence it is vital to compromise between maximum efficiency and efficiency at maximum power, that means to optimize between the efficiency and power of the heat engine.

Considerable attention has been devoted to the problem of the best mode of operation of heat engines working in finite time. Different criterion for the best performance of engine are reported in different works. Th ecriterion include power maximization, efficiency maximization, entropy generation minimization, minimization of loss of available work, etc [42 - 44]. The proper optimization criteria to be chosen for the optimum design of the heat engines may differ depending on their purposes and working conditions. If our main concern is not to obtain maximum work or power, but to have maximum benefit from energy, then the optimization objective is to get maximum efficiency. Fuel consumption is main concern for heat engines so the maximum thermal efficiency criterion is very important. If we are more concerned about power output, as it is the case of race car, maximum power output criterion is significant. If, like in the case of engines for transport purpose, both fuel consumption and time are equally important, then both the power and thermal efficiency criteria have to considered.

The optimal piston trajectories of an engine cycles for different optimization objectives have been studied by many researches. In 1991, Angulo-Brown introduced an ecological optimization criterion as an objective function to optimize the performance of a heat engine, taking in to account the maximum output power and the rate of production of entropy. In this study the author defines an objective function which gives the best compromise between high power output and low power loss. He showed that the production rate of entropy is greatly reduced by costing part of output power, when the optimum thermal efficiency is approximated to be the average of the respective Carnot efficiency

and Curzon-Ahlborn efficiency [45]. Shiyan Zheng and his co-worker report thier study on optimization of power output and efficiency of heat engine by using optimal control theory [46]. Mozurkewich and Berry described improved engine performance by optimized piston motion where they apply optimal control theory to optimize piston movement for the internal combustion engines [47, 48] whereas ecological function has been utilised to optimize diesel heat engine [49, 50]. These investigations are helpful to the optimal design and performance evaluation of heat engines.

Many performance analyses have been carried out based on two comparative criteria namely maximum power and maximum power density. Researchers involved in power maximization studies have utilized the thermal efficiency at maximum power [3] as an efficiency standard for practical heat engines. On the other hand, different studies showed that efficiency can be enhanced significantly by utilizing maximum power density criterion, while the power output from heat engines reduces. To compromise between the two, a new optimization criterion is introduced and supposed to work for all kind of heat engines [51]. The new criterion, called maximum efficient power, which is defined as the multiplication of power by efficiency, considers not only the power output, but also the cycle efficiency. Maximizing the efficient power gives a compromise between power and efficiency [25, 26, 27].

In reference [52] the authors applied an objective function proposed by A. C. Hernandez et. al. [51] to compute optimum efficiency. The proposed objective function works for any energy converter and expected to give best compromise between useful energy and lost energy. It is defined based on the concept of maximum efficient power optimization criterion and proved to be effective in optimizing between maximum efficiency and maximum power. And hence we used it to optimize the engine model considered in this study.

In general an objective function should satisfy the following conditions.

- Its dependence on the parameters of the process should be a guidance in order to

improve the performance of that process.

- It should not depend on the parameters of the environment (uncontroll parameters).
- It should take into account the unavoidable dissipation of energy provoked by the process.

An energy converter which produces a useful energy $E_u(x;\{\alpha\})$ from an input energy $E_i(x;\{\alpha\})$ by undertaking a thermodynamic process can have an efficiency given by

$$\eta(x;\{\alpha\}) = \frac{E_u(x;\{\alpha\})}{E_i(x;\{\alpha\})} \tag{2.5.1}$$

where x stands for independent variable while α represents a set of controll parameters. The efficiency $\eta(x;\{\alpha\})$ will have a value between minimum and maximum values of efficiency which is, respectively, defined as

$$\eta_{min}(\{\alpha\}) = \frac{E_{u,min}(x;\{\alpha\})}{E_i(x;\{\alpha\})} \tag{2.5.2}$$

$$\eta_{max}(\{\alpha\}) = \frac{E_{u,max}(x;\{\alpha\})}{E_i(x;\{\alpha\})} \tag{2.5.3}$$

Effective useful energy and lost useful energy can be defined respectively as follows

$$E_{u,eff}(x;\{\alpha\}) = E_u(x;\{\alpha\}) - \eta_{min}(\{\alpha\})E_i(x;\{\alpha\}) \tag{2.5.4}$$

$$E_{u,lost}(x;\{\alpha\}) = \eta_{max}(\{\alpha\})E_i(x;\{\alpha\}) - E_u(x;\{\alpha\}) \tag{2.5.5}$$

If the thermodynamic process is undertaken at a relatively large process rate, then only small fraction of useful energy can be extracted from a given amount of input energy, however if the process is taking place at a relatively slow process then there will be sufficient time to obtain a large amount of useful energy from the given amount of input energy. Thus to compromise between these two extremes one can define a new term Ω as the difference between effective useful energy and lost useful energy.

$$\begin{aligned} \Omega &= E_{u,eff}(x;\{\alpha\}) - E_{u,lost}(x;\{\alpha\}) \\ &= \frac{2\eta(x;\{\alpha\}) - \eta_{min}(\{\alpha\}) - \eta_{max}(\{\alpha\})}{\eta(x;\{\alpha\})} E_u(x;\{\alpha\}) \end{aligned} \tag{2.5.6}$$

Dividing both side by period(T) yields the rate dependence of eqn (4.2.12)

$$\frac{d\Omega}{dt} = \frac{2\eta(x;\alpha) - \eta_{min}(\alpha) - \eta_{max}(\alpha)}{\eta(x;\alpha)} \frac{dE_u(x;\alpha)}{dt} \tag{2.5.7}$$

Equation (4.2.13) is the objective function that we need to use to find the optimum path that gives the best compromise between effective useful energy and lost useful energy [51]. We can apply this equation to determine the value of the control parameter x that gives optimum performance of the heat engine model considered.

2.6 Motivation and Problem Statement

Heat engine is defined as a device that converts heat or thermal energy to mechanical (or other form of) work or more exactly a system which operates continuously and only heat and work may pass across its boundaries. A heat engine typically uses energy provided in the form of heat to do work and then exhausts the heat which can not be used to do work. The operation of a heat engine can best be represented by a thermodynamic cycle, since they operate in a cyclic manner, adding energy in the form of heat in one part of the cycle and using that energy to do useful work in another part of the cycle.

The First and Second Law of thermodynamics constrain the operation of a heat engine. The first law is the application of conservation of energy to the system, and the second sets limits on the possible efficiency of the machine and determines the direction of energy flow. The upper limit for the efficiency of any heat engine is the thermal efficiency of reversible Carnot cycle and it is called Carnot efficiency η_c which depends only on the temperatures of the reservoirs. However, it can only be achieved through the infinitely slow process required by thermodynamic equilibrium. Since it does not allow to obtain certain amount of power out put by using heat exchangers with finite heat transfer, Carnot efficiency does not have practical significance and is a poor guide for the performances of real heat engines.

A better approximation on the performance of real heat engine has been made by Curzon and Ahlborn by calculating efficiency of heat engine operating at its maximum power point, which is known as Curzon-Ahlborn efficiency η_{CA}. In their calculation, Curzon and Ahlborn consider the irreversibility of a linear finite rate heat transfer between the working fluid and its two heat reservoirs, though it is not the only source of irreversibility in real heat engines. Recently, different scholars are studying the effect of some more sources of irreversibility on the performance efficiency. The performance analysis of heat engine which involve some irreversibilities has been studied through employing various approaches of power maximization techniques and entropy generation minimization which is introduced by A. Bejan [19]. The establishment of this technique, also known as FTT, motivates many scholars to work on performance analysis of heat engine, optimization of finite time and finite rate processes and optimization of finite size devices. The optimization criteria used in these studies include power output, thermal efficiency and entropy generation [18-23]. The effect of engine size on the performance analysis is reported in [24] which introduce a new optimization criteria called maximum power density (the ratio of power to the maximum specific volume in the cycle). More efficient optimization criterion called maximum efficient power, which considers both power output and efficiency, has been applied to study a heat engine operating with Carnot-like cycle [25, 26, 27]. In 2008 G. Aragon-Gonzalez et. al. reported their study about the optimization of power output and efficiency of irreversible Carnot cycle by considering internal temperature ratio and time ratio for the heat exchange as parameters for the optimization [15]. In the same year Y. Izumuda and K. Okuda studied finite-time Carnot cycle of weakly interacting gas and, for the first time, they verified the validity of η_{CA} numerically using MD simulation technique [32].

The global climate is being changed at an alarming rate due to increasing emission of green house gases (GHG). It is the accelerating petroleum consumption of the world that is mainly responsible for the increasing emission of GHG. The transport sector has

significant contribution to the total CO_2 emission to the environment. Emission of CO_2 from the transport sector is still growing rapidly due to the expansion in the transport sector. More over the world is getting more concerned about the energy supply base which is largely on foreign oil and has led to uncertainity on the stability of fuel price on the global market. Due to these and similar factors the automotive industries are forced to increase its focus on developing feul efficient vehicles. The study report in Massachusetts Institute of Technology (MIT) [53] shows that 30 - 50 percent of fuel consumption can be reduced by improving gasoline and deisel engines and transmissions, gasoline hybrids and reduction in vehicle weight. It also shows the problem of growing transportation fuel use and GHG emissions can be solved mainly by developing more efficient vehicles. In general the growing global energy demand, concern about energy supply base, unstability on the fuel price in the global market and environmental concerns has increase the demand for fuel efficient vehicles.

The vast majority of motors that power our planes, trains, and automobiles are heat engines. They rely on the rapid expansion of gas as it heats up to generate movement. Different types of heat engines use different source of heat, but all of them are unable to utilize 100 percent of the supplied energy, rather part of it will be exhausted. Actually real heat engines waste a large amount of heat energy. Hence modern energy conversion technologies should combine high conversion efficiencies with low emissions, especially careful consideration for CO_2 emission. As a consequence, accurate design methods and optimal device energy performance of the conversion technologies are required. Device design and performance optimization are among the central issues in modern technology. Generally, due to the need of a sustainable supply of energy and due to strong concerns about the environmental impact of the combustion of fossil fuels, performance efficiency of thermal engines remains a central issue in physics [54]. All these facts encourage and motivate us to work on performance analysis and optimization of heat engine. Since, to the best of our knowledge, no work is reported on the performance analysis of heat engine

considering the possible intermolecular interaction in the working gas, we start to study the thermodynamic process in the working substance of a heat engine where the working substance is considered to be real gas. In this work we focus on studying the performance of a heat engine operating with Carnot like cycle where we have used process rate and temperature ratio of the reserviors to be control parameters. The study is carried with the aid of computer experiment where we apply classical MD simulation technique. We have also apply unified optimization criterion to find optimum values for efficiency and power output per cycle for the model engine considered.

2.7 Objective of The Study

The main objective of this work is to study finite-time thermodynamics of heat engine where the working fluid is a real gas. We have also the following specific objectives:

1. To study an endoreversible heat engine operating with a carnot like cycle by employing MD simulation technique.

2. Measuring the efficiency of heat engine of real gas with computer simulation.

3. Determining the power and efficiency of the engine for a wide range of process rates and temperature ratios of the reserviors.

4. Determining the values for maximum efficiency and efficiency at maximum power.

5. To find an optimum path for the thermodynamics process in the working gas which gives the best compromise between maximum efficiency and efficiency at maximum power.

2.8 Methodology of The Study

The extremely powerful technique to study matter at the atomistic level is Molecular Dynamics Simulation. The nature of matter is based on the structure and motion of its

constituent particles or molecules. The dynamics of these constituent building blocks can be studied by solving classical N-body problem, which can only be solved numerically. Hence, the study of matter at the atomistic level require computational tools which allow to follow the movement of individual molecules. This is what MD simulation technique is intended to do [55 - 61].

Given the form of the interparticle potential, we can determine the total force on each particle due to all the other particles in the system. Given this force, we find the acceleration of each particle from Newtons second law of motion. Because the acceleration is the second derivative of the position, we need to solve a second-order differential equation for each particle (for each direction). (For a three-dimensional system of N particles, we would have to solve 3N differential equations.) These differential equations are coupled because the acceleration of a given particle depends on the positions of all the other particles. Obviously, we cannot solve the resultant set of coupled differential equations analytically. However, we can use relatively straightforward numerical methods to solve these equations to a good approximation. This way of simulating dense gases, liquids, solids, and biomolecules is called molecular dynamics simulation. And we found that MD simulation technique is the appropriate way to study the finite-time thermodynamics of the heat engines, hence we use it exhuastively in our project. MD simulation technique is briefly introduced in chapter 2.

Chapter 3

Molecular Dynamics Simulation

3.1 Introduction

The advent of high speed computers altered the traditional relationship between theory and experiment by inserting a new element right in between, computer experiment. In the previous years physical sciences were characterised by an interplay between experiment and theory. In experiment, a system is subjected to measurements, and results, expressed in numeric form, are obtained. In theory, a model of the system is constructed, usually in the form of a set of mathematical equations. The model is then validated by its ability to describe the system behavior in a few selected cases, simple enough to allow a solution to be computed from the equations. However, the problem is made to be solvable through a considerable amount of simplification in order to eliminate all the complexities invariably associated with real world problems.

Theoretical models are usually tested only in a few simple special circumstances. For example, a model for intermolecular forces in a specific material could be verified in a diatomic molecule, or in a perfect, infinite crystal, which still require employing more aproximation to carry out the calculation. However, many physical problems of extreme interest (like physics and chemistry of defects, surfaces, organic molecules, disordered systems, etc) fall outside the realm of these special circumstances. Hence a new technique, computer experiment, is introduced to handle such complex physical problems.

In computer experiment, though the model is still developed by theorists, calculations are carried out by machine following certain algorithm. And hence complexity can be introduced and more realistic systems can be investigated. Computer simulation took advantage over theory through increasing the demand for accuracy of the models and being very close to experimental conditions, to the extent that computer results can sometimes be compared directly with experimental results. Hence simulation becomes an extremely powerful tool not only to understand and interpret the experiments at the microscopic level, but also to study regions which are not accessible experimentally, or which would imply very expensive experiments [55, 56, 57].

Computer simulation is used to understand the properties of assemblies of molecules in terms of their structure and the microscopic interactions between them. This serves as a complement to conventional experiments, enabling us to learn something new, something that cannot be found out in other ways. Computer simulations act as a bridge between microscopic length and time scales and the macroscopic world of the laboratory: we provide a guess at the interactions between molecules, and obtain good predictions of bulk properties. Hence it can be used to study, characterize and predict properties of macroscopic system by studying microscopic model. Moreover it can also serve as a bridge between theory and experiment. Unlike that of a traditional theory which is based on reductionistic approach, where we deal with complexity by reducing a sytem to simpler subsystems that are simple enough to be represented with solvable models, computer simulation is used as a practical tool to computationally verify and test models in situations which are too complex to handle analytically. We may test a theory by conducting a simulation using the same model. We may test the model by comparing with experimental results. We may also carry out simulations on the computer that are difficult or impossible in the laboratory (for example, working at extremes of temperature or pressure). Computer simulation technique consists of two main branches; Molecular Dynamics (MD) and Monte Carlo (MC).

The Monte Carlo method is a stochastic strategy that relies on probabilities. The Monte Carlo sampling technique generates large numbers of configurations or microstates of equilibrated systems by stepping from one microstate to the next in a particular statistical ensemble. Random changes are made to the positions of the species present, together with their orientations and conformations where appropriate. Quantities of interest can be averaged over these microstates. The advantages of the Monte Carlo simulation technique include the ease of extending it to simulate different ensembles, flexibility in the choice of sampling functions and the underlying matrix or trial move which must satisfy the principle of microscopic reversibility as well as time saving as only the potential energy is required [58].

MD simulation is a computer simulation technique where the time evolution of a set of interacting atoms is followed by integrating their equations of motion. MD simulation consists of the numerical, step-by-step, solution of the classical equations of motion. It is the most detailed molecular simulation method which computes the motions of individual molecules. In MD simulation coupled Newtons equations of motion, which describe the positions and momenta, are solved for a large number of particles in an isolated cluster or in the bulk using periodic boundary conditions. The equations of motion for these particles which interact with each other via intra- and inter-molecular potentials can be solved accurately using various numerical integration methods such as predictor-corrector or Verlet methods. MD simulation follows the laws of classical mechanics [55 - 60], and most notably Newton's law of motion

$$\mathbf{F}_i = m_i \mathbf{a}_i \tag{3.1.1}$$

for each atom i in a system containing N atoms, where $\mathbf{F}_i$ is the force acting up on the i^{th} atom, due to the interactions with other atoms. Therefore, in contrast with the Monte Carlo method, MD is a deterministic technique: given an initial set of positions and velocities, the subsequent time evolution is in principle completely determined. Molecular dynamics efficiently evaluates different configurational properties and dynamic quantities

which cannot generally be obtained by Monte Carlo. MD simulation technique takes the advantage over MC in that it gives a route to dynamical properties of a system; transport coefficients, time-dependent responses to perturbations, spectra, etc [59].

Molecular dynamics merges computer simulation with statistical mechanics to compute equilibrium and transport properties of a classical many-body system. Equilibrium properties include the energy, temperature and pressure of a system. Transport properties include the diffusion coefficient, shear viscosity and thermal conductivity of a system. Molecular dynamics simulations take place in three steps. First, we specify the initial positions and momenta of the particles. The particles interact through a potential. So the implemented potential determines the extent to which our simulation results represent the system of interest. Second, we evolve the system according to Newton's law: $\mathbf{F}_i = m_i\mathbf{a}_i$. Visually, the particles move around in the simulation box, tracing out trajectories in space. Third we measure physical quantities as functions of particle positions and momenta. Statistical mechanics is applied to interpret these instantaneous measurements in terms of equilibrium properties. In statistical mechanics, a macroscopic property of a system is an average of that property over all possible Quantum states. This is referred to as an ensemble average. The ergodic hypothesis states that the time-averaged properties of a real system are equal to its ensemble averages. So by taking the average of measurements in a molecular dynamics simulation, we can obtain the macroscopic properties of the system. Transport properties can also be computed from the data because the complete trajectories are available. They are defined in terms of time-dependent correlation functions at the atomic level [60].

MD simulation in general involves the following four steps.

Starting the simulation

MD simulation is usually started from defining a simulation box and initial configuration of the particles constituting the system. Initial positions of the particles can be defined

either randomly or on a lattice. The later approach is more common since it avoids any possible overlap between particles and hence obey Pauli exclusion principle. Then we set initial velocities for each of the particles. The initial velocities can be taken to be zero or generated from Maxwellian distribution function depending up on our interest and the type of the system we are dealing with. Actually, this kind of initial state may not correspond to an initial condition. But, once the simulation is started, equilibrium is usually reached with in hundreds or few thousands of simulation time steps. Before starting the simulation, however, some randomization must be introduced in order to avoid symmetry between the atoms that can be possibly introduced during the initial configuration, especially if it is defined on a lattice. Otherwise the equations of motions of the particles that are symetrically equivalent will lead the particles to evolve exactly the same way, or the net force on the particles could vanish and the atoms would sit idle indefinitely. The randomization can be done either by randomly displacing the particles from their lattice positions through small displacement or taking the initial velocities assigned to the particles from a Maxwell distribution function at a certain temperature T. If the latter approach is chosen, one should be certain that the linear momentum of the total system vanish which can be through subtracting average velocity from velocities of each particles.

Running the simulation

After having a well defined model of a system with initial configuration and randomized initial velocities of each particles constituting the system, the next step is just to run the simulation. In this part the most time consimung part of the simulation, calculating forces on each particles and following the time evolution of the particles, is performed.

Equilibration

Thermodynamic equilibrium state of a system can be altered whenever state of the system changes. At this time thermodynamic parameters of the system are not anymore constant,

rather they fluctuate about some value for a while before relaxing to a new value. Change in state of the system can be introduced in a planned manner by the researcher or it can happen spontaneously. Any one can change state of a system by changing some simulation parameters like temperature or density of the system. The spontaneous change can be introduced when the system undergoes phase transition. What ever the case for disturbance of the system under consideration from its equilibrium state, one should wait until the system relaxes to a new equilibrium state before starting to take measurments on the system. In general, equilibrium of a system takes place exponentially with time and hence relaxation time usually is in the order of hundreds or few thousands of simulation time steps.

Taking measurements

Once equilibration of the system is achieved, one can measure any statistical quantities of the system. The measurements can be taken by performing time averages of physical properties over the system trajectory.

3.2 Modeling a Physical System

The main ingredient of a simulation is a model for the physical system. For a molecular dynamics simulation this amounts to choosing the potential: a function $U(\mathbf{r}_1, ..., \mathbf{r}_N)$ of the positions of the nuclei, representing the potential energy of the system when the atoms are arranged in that specific configuration. Forces are then derived as the gradients of the potential with respect to atomic displacements

$$\mathbf{F}_i = -\nabla_{\mathbf{r}_i} U(\mathbf{r}_1, ..., \mathbf{r}_N) \tag{3.2.1}$$

The potential energy due to non-bonded interactions between N particles is a function of the positions of particles nuclei and can be given by

$$U(\mathbf{r}_1, ..., \mathbf{r}_N) = \Sigma_i U(\mathbf{r}_i) + \Sigma_i \Sigma_{j>i} U(\mathbf{r}_i, \mathbf{r}_j) + \Sigma_i \Sigma_{j>i} \Sigma_{k>j} U(\mathbf{r}_i, \mathbf{r}_j, \mathbf{r}_k) + ... \tag{3.2.2}$$

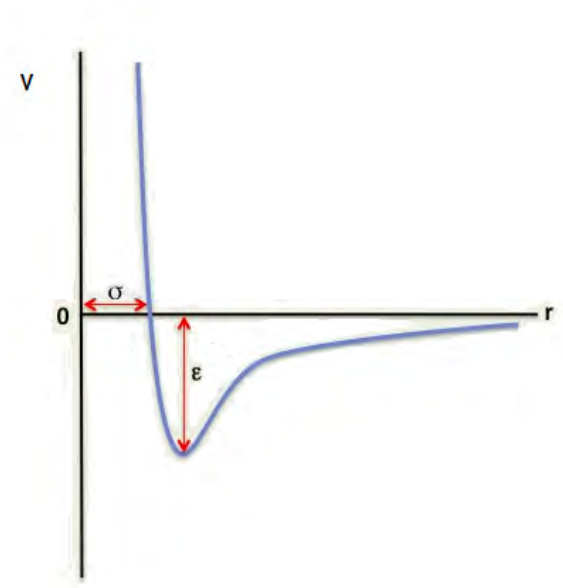

Figure 3.1: Lennard-Jones Potential

where $U(\mathbf{r}_i)$ represents the effect of an external field (including the container walls), $U(\mathbf{r}_i, \mathbf{r}_j)$ represents pairwise interactions and $U(\mathbf{r}_i, \mathbf{r}_j, \mathbf{r}_k)$ represents three-body interactions. In the absence of external field the major contribution to the potential is due to pair interaction which depends only on the magnitude of pair separation $\mid \mathbf{r}_i - \mathbf{r}_j \mid$. Hence for the simplest model U can be written as the sum of pairwise interactions, provided that there is no external force acting on the system

$$U(\mathbf{r}_1, ..., \mathbf{r}_N) = \Sigma_i \Sigma_{j>i} U(\mid \mathbf{r}_i - \mathbf{r}_j \mid) \tag{3.2.3}$$

The condition $j > i$ in the second summation of the above equation is introduced to prevent repeated consideration of any pair interaction. In pairwise interaction, we use, most commonly, Lennard-Jones potential which initially was proposed for liquid argon

$$U_{LJ}(r) = 4\varepsilon[(\frac{\sigma}{r})^{12} - (\frac{\sigma}{r})^{6}] \tag{3.2.4}$$

where σ is atomic diameter and ε is the potential well depth as shown in Fig. 3.1.

This potential is strongly repulsive at short distances which is represented by r_{ij}^{-12} term to model the strong repulsion due to the non-bonded overlap of the electronic orbitals. The repulsion arises from two effects. First, the penetration of one electron shell by another; the nuclear charges are no longer completely screened, and therefore repel one another. Second, Pauli's exclusion principle, which states that two electrons of the same energy cannot occupy the same element of space. So when electron shells overlap, the energy of one must be increased, and this is equivalent to a force of repulsion. It has arbitrary form but the exponential is more appropriate and it has no theoretical justification [61]. The attractive term, r_{ij}^{-6}, dominates at large distances and it models the van der Waals dispersion forces caused by the dipole-dipole interactions due to fluctuating dipoles. These weak forces are responsible for the bonding character of closed-shell systems. Hence Lennard-Jones potential is inadequate for open shell systems in which strong localized bonds are formed. The potential in eqn (3.2.4) has an infinite range. This results in high computational cost in the simulation process due to considering all atomic pairs in the system. To simplify the program and to save enormous amount of computer resources it is customory to establish a cut off radius r_c and disregard the interactions between atoms separated by more than r_c. The potential is often shifted in order to vanish at the cutoff radius to avoid energy jump at that point and keep energy conservation. The shifted potential is then written as

$$\begin{aligned} U(r) &= U_{LJ}(r) - U_{LJ}(r_c) \text{ if r} \leq r_c \\ &= 0 \text{ if r} \geq r_c \end{aligned} \tag{3.2.5}$$

The inter-particle forces arising from the Lennard-Jones potential is then

$$f_{ij} = \frac{48\varepsilon}{r_{ij}^2}[(\frac{\sigma}{r_{ij}})^{12} - \frac{1}{2}(\frac{\sigma}{r_{ij}})^6]\mathbf{r}_{ij} \tag{3.2.6}$$

The most time consuming part of a molecular dynamics simulation is calculation of the forces on the atoms. For a system of N atoms, the forces are computed by sampling

$\frac{1}{2}N(N-1)$ unique r_{ij} distances at each time step of the simulation. Here r_{ij} is the separation distance between atoms i and j. When a truncated potential is used, the force equals zero for any $r_{ij} > r_c$; consequently evaluating distances r_{ij} that are greater than r_c wastes computer time. However, one can improve the speed of a program by minimizing the number of pairs whose separation distance shall be evaluated. This can be done by using either Verlet neighbour list method or cell linked list method. In the Verlet neighbour list method we use lists of nearby pairs of atoms. The potential cutoff sphere, of radius r_c , around a particular atom is surrounded by a skin, to give a larger sphere of radius r_m as shown in Fig. 3.2. At the first step in a simulation, a list is constructed of all the neighbours of each atom, for which the pair separation is within r_c. Over the next few MD time steps, only pairs appearing in the list are checked in the force routine. From time to time the list is reconstructed: it is important to do this before any unlisted pairs have crossed the safety zone and come within interaction range. On the other hand, in the cell linked list method the simulation box will be divided in to n_{cell} cells whose side $l_{cell} = \frac{L}{n_{cell}}$ should be greater than r_c Fig. 3.3. If there is a separate list of atoms in each of those cells, then searching through the neighbours is a rapid process: it is only necessary to look at atoms in the same cell as the atom of interest, and in nearest neighbour cells. This approach is very efficient for large systems with short-range forces [55,58].

3.3 Periodic Boundary Condition

The other challenge of MD simulation is a surface effect. The behavior of finite systems is very different from that of massive systems, hence the number of particles used to simulate bulk properties of macroscopic systems plays an essential role. In massive systems, only a small fraction of the atoms are located in the vicinity of the boundaries, or the fraction of particles near the walls is negligible. MD is typically applied to systems containing several hundereds or a few thousand atoms. No matter how large the simulated system is, its number of atoms would be negligible compared with the number of atoms contained

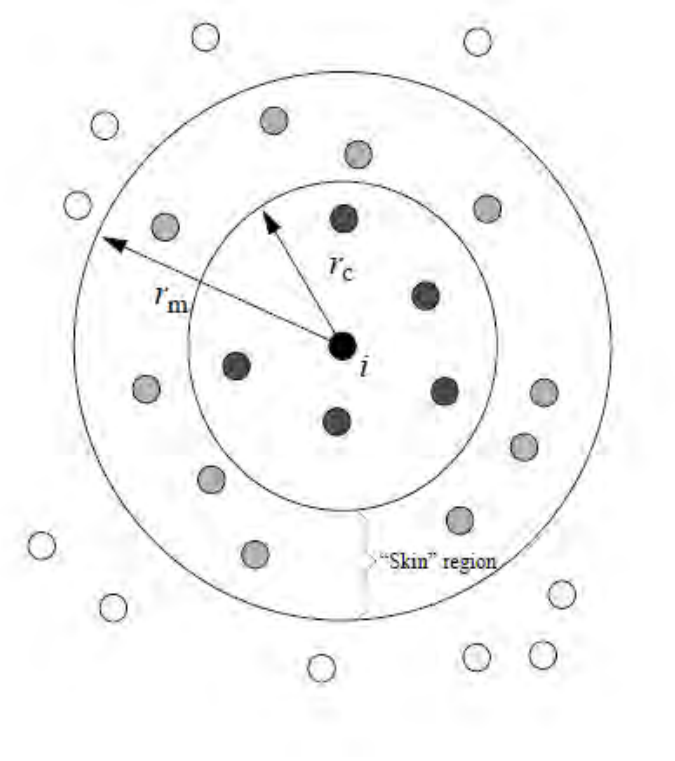

Figure 3.2: Neighbours of an atom can be searched only in the sphere of radius r_m[58]

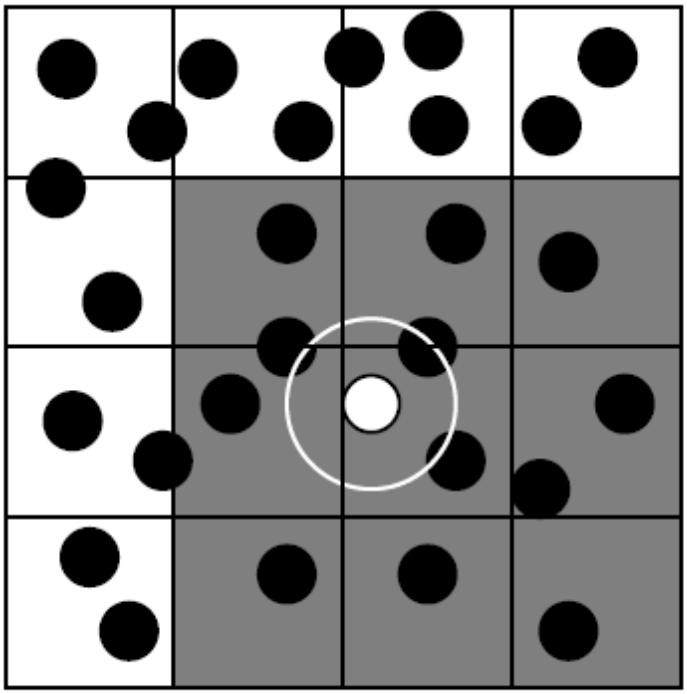

Figure 3.3: Neighbours of an atom can be searched by examining atom's own cell and neighbour cells alone[58]

in a macroscopic peice of matter which is in the order of Avogadro's number, and the ratio between the number of surface atoms and the total number of atoms would be much larger than in reality, causing surface effects to be much more important than what they should do. To remove these surface effects it is customary to introduce periodic boundary condition which can be done by surrounding the box with replicas of itself as shown in Fig. 3.4. Using periodic boundary condition means particles enclosed in a box are mentally replicated to infinity by rigid translation in all the three cartesian coordinates, completly filling the space. This means if one particle is located at position **r** in the box, one can assume that this particle realy represents an infinte set of particles located at

$$\mathbf{r} + a\mathbf{i} + b\mathbf{j} + c\mathbf{k} \tag{3.3.1}$$

where a, b and c are integers and **i**, **j** and **k** are unit vectors along each three edges of the box [56, 58]. All these image particles move together with their original particle, and in fact only one of them is effectively simulated. When a particle enters or leaves the simulation region, an image particle leaves or enters the region such that the number of particles in the simulation region is always conserved. In other word, in the course of the simulation, if an atom leaves the basic simulation box, attention can be switched to the incoming image [8]. In the case where periodic boundary condition is applicable, the coordinates of the particles under consideration must be examined at each integration step. If a particle is found to have left the simulation region, its coordinates must be readjusted to bring it back inside, which is equivalent to shift the focus to the image of the particle which enters the simulation region through the opposite boundary. Supposing that the simulation region is a rectangular box, this is done by adding/subtracting the size L of the box to/from the cooresponding coordinate of the particle found to have left the simulation region. The choice of addition or subtraction is based on whether the cooresponding coordinate of the particle is less than zero or greater than L respectively. For example, considering the x-coordinate of a particle and assuming that the size of the simulation box along x-axis is L_x, the particle's coordinate can be reajusted as follows

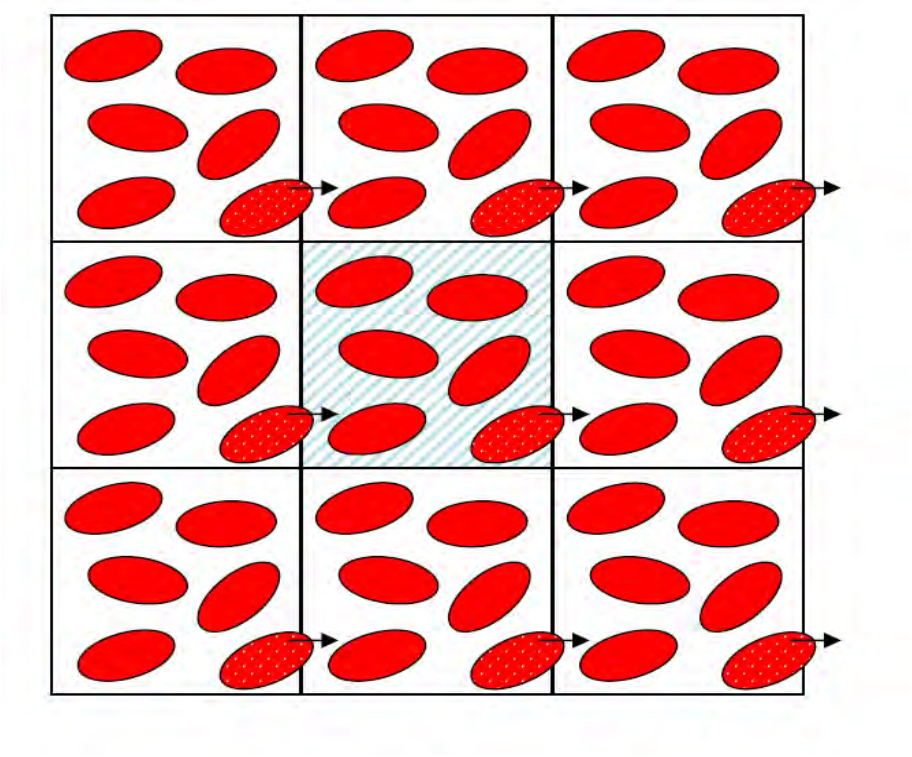

Figure 3.4: Any particle which leaves the simulation box replaced by its image

$$x \longrightarrow x + L_x \text{ if x} < 0$$
$$x \longrightarrow x - L_x \text{ if x} > L_x \tag{3.3.2}$$

In the case where periodic boundary condition is aplicable, each particle i in the box should be thought of as interacting not only with other particles j in the box, but also with their images in nearby boxes which, as a consequence, increases the number of interacting pairs enormously. However, this chalenge can be solved by applying minimum image convention.

3.4 Minimum Image Criterion

As a result of using periodic boundary conditions, each particle i in the simulation box appears to be interacting not only with the other particles in the box, but also with their

images. Apparently, the number of interacting pairs increases enormously. Nevertheless, this inconvenience can be overcome if one uses a potential with a finite range, since the interaction of two particles separated by a distance exceeding a cutoff distance r_c can be ignored. Provided the potential range is not too long, we can adopt the minimum image convention that each atom interacts with the nearest atom or image in the periodic array. Supposing that the box size is larger than $2r_c$ along each Cartesian direction, it is obvious that at most one among the pairs formed by a particle i in the box and all the periodic images of another particle j will lie within the cut off distance r_c and, thus, will interact, and this can prevent the increment in the number of interacting pairs as an effect of periodic boundary condition. This is called the minimum image criterion: among all images of particle j, particle i interacts with only the closest and neglect the rest [55, 58].

3.5 Time Integration Algorithm

The engine of a molecular dynamics program is its time integration algorithm, required to integrate the equation of motion of interacting particles. It is based on finite difference method. The integration algorithm is aimed at knowing the positions and their time derivatives of the particles at time $t + \Delta t$ based on their quantities at time t. Iterating the procedure allows to follow the time evolution of the system. Since the schemes are aproximate, the method is suscebtible to truncation and round of errors, but both of them can be reduced by decreasing Δt.

Altough there are different types of time integration algorithms, in MD the most commonly used algorithm is velocity Verlet algorithm. Equations for advancing positions and velocities are written as follow, [55 - 60]

$$\mathbf{r}(t + \Delta t) = \mathbf{r}(t) + \Delta t\mathbf{v}(t) + \frac{1}{2}(\Delta t)^2\mathbf{a}(t) \tag{3.5.1}$$

$$\mathbf{v}(t + \frac{1}{2}\Delta t) = \mathbf{v}(t) + \frac{1}{2}\Delta t\mathbf{a}(t) \tag{3.5.2}$$

$$\mathbf{a}(t+\Delta t) = -\frac{1}{2}m\nabla U(\mathbf{r}(t+\Delta t)) \tag{3.5.3}$$

$$\mathbf{v}(t+\Delta t) = \mathbf{v}(t+\frac{1}{2}\Delta t) + \frac{1}{2}\Delta t\mathbf{a}(t+\Delta t) \tag{3.5.4}$$

Chapter 4

Model Description

4.1 Model of The System

In this work we simulate the cyclic thermodynamic process in the working gas of a heat engine operating with a Carnot-like cycle between two resevoirs of temperature T_c and T_h. This chapter is then devoted to discuss the model we use for our simulation study and some of the statistical quantities measured during the course of the simulation.

4.1.1 Initial Configuration

We model a cubic box of length L containing N identical gas molecules of mass m. The molecules inside the cubic box are initially configured with fcc lattice structure, just to avoid overlaping. Then all the molecules are given random initial velocity which melts the system and molecules can move randomly inside the cylinder and hence behave as gas molecules. The initial velocities are chosen randomly from the Maxwell-Boltzman distribution function [62]

$$f(\mathbf{v})d\mathbf{v} = (\frac{m}{2\pi k_B T})^{\frac{3}{2}} \exp{(\frac{-m\mathbf{v}^2}{2k_B T})}d\mathbf{v} \tag{4.1.1}$$

where $f(\mathbf{v})d\mathbf{v}$ is the mean number of molecules whose center of mass velocity lies between $\mathbf{v}$ and $\mathbf{v} + d\mathbf{v}$, m is mass of the molecule, k_B is Boltzman constant and T is temperature of the system. The velocities were corrected so that there was no overall momentum by setting the center of mass velocity equal to zero. This prevents the system from drifting in

space. Then after, the movement of the molecules is governed by the interaction between the molecules themselves. The nature of interaction between the molecules is assumed to be pair interaction which depends only on the intermolecular separation which can be well represented by Lennard-Jones potential, the only potential we consider in our system

$$U^{LJ}(r) = 4\varepsilon[(\frac{\sigma}{r})^{12} - (\frac{\sigma}{r})^{6}] \tag{4.1.2}$$

where r is intermolecular separation, ε is the depth of the potential well and σ is the finite distance between two molecules at which intermolecular potential is zero. Since identical molecules are considered, the potential due to intermolecular interaction depends only on the intermolecular separation. Hence, our model can be considered as a system consisting of N neutral molecules, whose internal structure can be ignored, enclosed in a container of volume V where the container is assumed to be far from the influence of any external field, like gravity. The motion of the molecules is then given by classical mechanics, Newton's second law of motion. In principle, it is possible to follow the trajectory of each molecule and the evolution of the system by combining initial configuration and initial velocities of the molecules with equations of motion of each molecules.

One of the box sides is made to be a moveable piston whereas the opposite side is a thermalizing wall as shown in Fig. 4.1. The piston is allowed to move at a certain speed where the piston speed is considered to be a control parameter and hence can be used as a parameter to optimize the efficiency of the engine. Usually we want to simulate a large size system of gas or liquid. In such systems the fraction of molecules near the walls of the container is negligibly small. However, the number of molecules that can be studied in a simulation is typically in the order of hundreds, thousands or few hundred thousands. For these relatively small systems, the fraction of molecules near the walls of the container would be significant, and hence the behavior of such a system would be dominated by surface effects. The most common way of minimizing surface effects and to simulate more closely the properties of a macroscopic system is to use periodic boundary conditions. Thus, at the walls of the box, except for the piston and thermalizing wall,

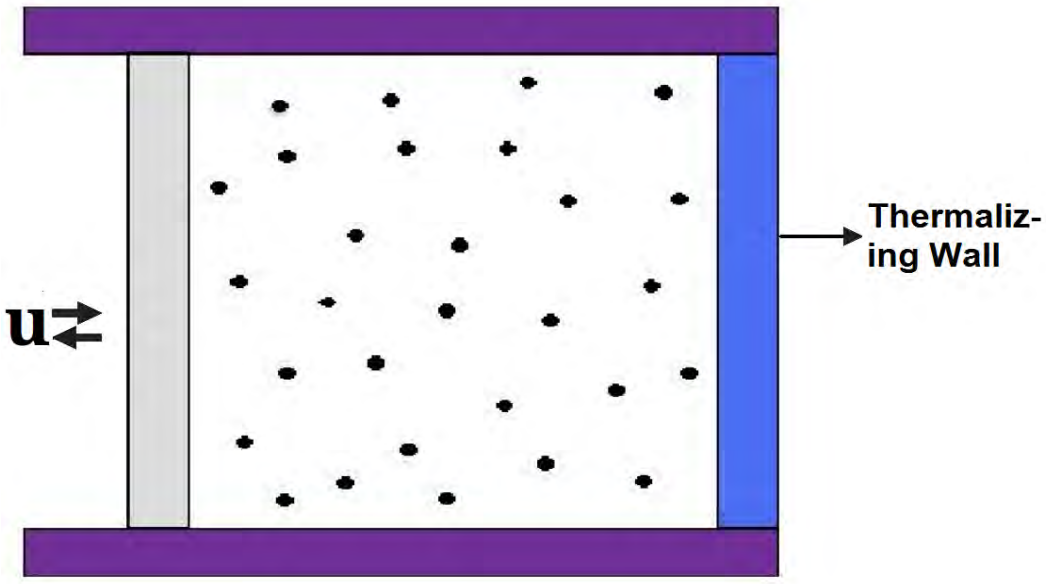

Figure 4.1: Cross-sectional view of the model

periodic boundary condition is applied.

4.1.2 Interaction of Gas Molecules With The Moving Piston

The compression and expansion steps of the cyclic thermodynamic processes in the working gas is considered by letting the piston to move back and forth with a constant speed u. When a molecule of velocity $\mathbf{v} = (v_x, v_y, v_z)$ collides with the piston moving along x-axis with velocity u, the new x-component of the velocity of the molecule is obtained assuming perfectly elastic collision between the piston and the colliding molecule. By applying conservation of momentum and kinetic energy along x-axis [63] one can write; for conservation of momentum

$$mv_x + Mu = mv'_x + Mu'$$
$$m(v_x - v'_x) = M(u - u') \tag{4.1.3}$$

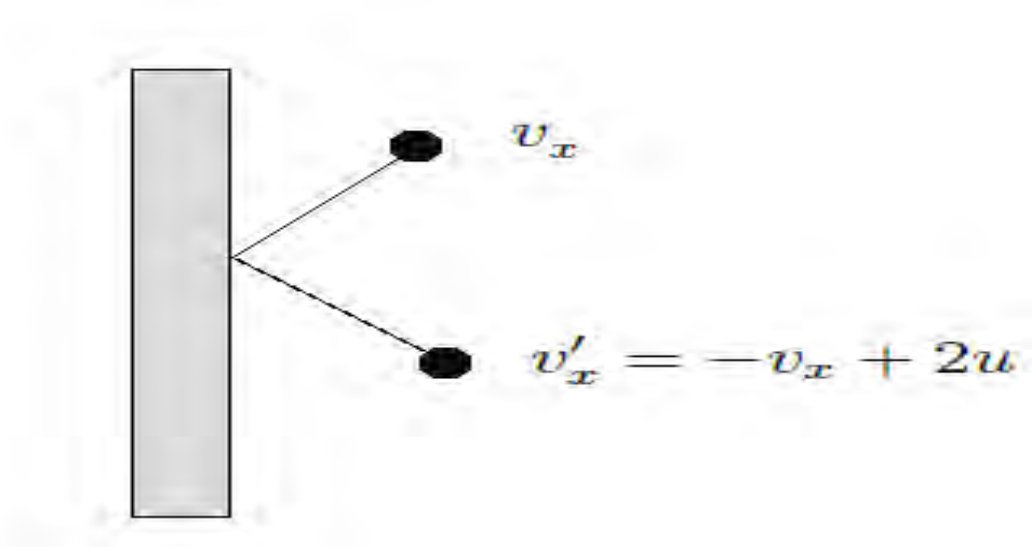

Figure 4.2: Model For Gas Molecule-Piston Interaction

and for conservation of kinetic energy

$$\frac{1}{2}mv_x^2 + \frac{1}{2}Mu^2 = \frac{1}{2}mv_x'^2 + \frac{1}{2}Mu'^2$$
$$m(v_x^2 - v_x'^2) = M(u'^2 - u^2)$$
$$m(v_x - v_x')(v_x + v_x') = M(u' - u)(u' + u)$$
$$v_x' = -v_x + 2u \tag{4.1.4}$$

where we assume the collision doesn't significantly affect the speed of the piston $u \simeq u'$ and we use eqn (4.1.3). In these equations m and M represent masses of the molecule and the piston respectively. Similarly when the gas molecule of velocity $\mathbf{v} = (v_x, v_y, v_z)$ collides with the piston moving along x-axis with speed $-u$, the x component of the velocity of the gas molecule changes to

$$v_x' = -v_x - 2u \tag{4.1.5}$$

Thus when a molecule of velocity $\mathbf{v} = (v_x, v_y, v_z)$ collides with the piston moving along x-axis with velocity $\pm u$, the velocity of the gas molecule changes to

$$\mathbf{v}' = (-v_x \pm 2u, v_y, v_z) \tag{4.1.6}$$

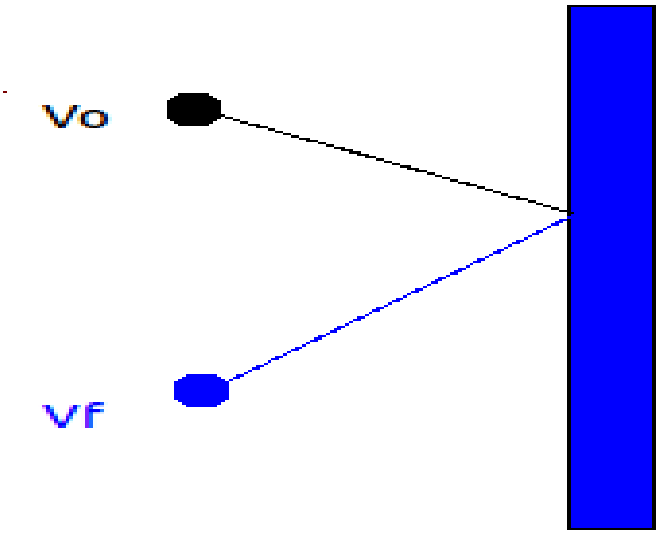

Figure 4.3: Model For Gas Molecule-Wall Interaction

4.1.3 Interaction of Gas Molecules With The Thermalizing Wall

The working substance is set to be in thermal contact with a thermalizing wall of temperature $T_h(T_c)$ to consider the heat intake (exhaust) when it undergoes isothermal expansion (compression). The thermalizing wall is considered to be a static system consisting of a large number of identical molecule (molecule reservoir) which resembles the gas molecules and whose velocities are governed by Maxwell-Boltzmann distribution at temperature T_i, hence mean number of molecules per unit volume with the center of mass velocity between $\mathbf{v}$ and $\mathbf{v}$ + d$\mathbf{v}$ is given by

$$f(\mathbf{v}, T_i)d\mathbf{v} = (\frac{m}{2\pi k_B T_i})^{\frac{3}{2}} \exp{(\frac{-m\mathbf{v}^2}{2k_B T_i})}d\mathbf{v} \tag{4.1.7}$$

where k_B is Boltzman constant, i = h(c) when the working substance is in thermal contact with the thermalizing wall of temperature $T_h(T_c)$. Then a gas molecule in the cylinder

which collides with the thermalizing wall is assumed to be replaced by a randomly selected molecule from the molecule reservoir. Thus the velocity of the new molecule which comes from the molecule reservior in to the cylinder is governed by a velocity distribution function proportional to the Boltzmann factor multiplied by $-v_x$. The mean number of molecules per unit volume replaced in the cylinder with the center of mass velocity between $\mathbf{v}$ and $\mathbf{v}$ + d$\mathbf{v}$ is then

$$f(\mathbf{v}, T_i)d\mathbf{v} = C(-v_x)\exp\frac{-mv^2}{2k_BT_i}d\mathbf{v} \tag{4.1.8}$$

The proportionality constant C can be determined from normalization condition and hence the value of the center of mass velocity of these molecules is governed by the distribution function

$$f(\mathbf{v}, T_i)d\mathbf{v} = \frac{1}{2\pi}(\frac{m}{k_BT_i})^2 v_x \exp\frac{-mv^2}{2k_BT_i}d\mathbf{v} \tag{4.1.9}$$

In other way the gas-wall interaction is modeled in such a way that as a gas molecule strikes the thermalizing wall, all the three components of velocity of the molecule are reset to a biased Maxwellian distribution and the direction of the x-component velocity is set to be away from the wall [32, 65]. A gas molecule is said to strike the wall when the center of mass position of the gas molecule is closer to the internal surface of the wall with a distance less than 0.5σ.

4.1.4 Heat Exchange Between The Reservoirs And Working Substance

The amount of heat flowing from the hot reservior to the gas, during isothermal expansion, and from the gas to the cold reservior, during isothermal compression, is calculated from the sum of change in kinetic energy of the molecules during collision with the thermalizing wall. During isothermal expansion the system is set to be in thermal contact with the hot reservior. This means the thermalizing wall is at higher temperature than the system, and hence molecules in the molecule reservior, in general, have larger kinetic energy than the gas molecule, $v'^2 > v^2$. Thus due to the change in momentum (or due to molecule

replacement in the cylinder) during collision, the working gas gains energy in the form of heat, or heat flow takes place from the thermalizing wall at higher temperature to the working gas at lower temperature. The amount of heat energy H_1 flowing from the hot reservoir to the system is then the sum of change in kinetic energy of the gas molecules

$$H_1 = \frac{1}{2}m\sum_i (v_i'^2 - v_i^2) \tag{4.1.10}$$

while during isothermal compression the system is set to be in thermal contact with the cold reservior where $v'^2 < v^2$. The amount of heat energy H_2 flowing from the system to the cold reservior is then

$$H_2 = \frac{1}{2}m\sum_i (v_i^2 - v_i'^2) \tag{4.1.11}$$

The net heat H_{net} flowing from the reservior to the system, which is equal to the work done W by the system, per cycle becomes

$$H_{net} = W = H_1 - H_2 \tag{4.1.12}$$

The efficiency of the engine is then computed as

$$\eta = \frac{W}{H_1} = \frac{H_1 - H_2}{H_1} \tag{4.1.13}$$

Here it should be noted that we use average values of W, H_1 and H_2 for certain number of complete cycle processes.

4.1.5 The Volume Proportion For Adiabatic And Isothermal Processes

The usual carnot cycle consists of four processes: Isothermal expansion ($V_1 \to V_2$), Adiabatic expansion ($V_2 \to V_3$), Isothermal compression ($V_3 \to V_4$) and Adiabatic compression ($V_4 \to V_1$) where $V_i s$ are as shown in figure 1. This section is devoted to discuss how the volume proportion for each branches of the cycle considered, i.e., obtaining the values of $V_i s$.

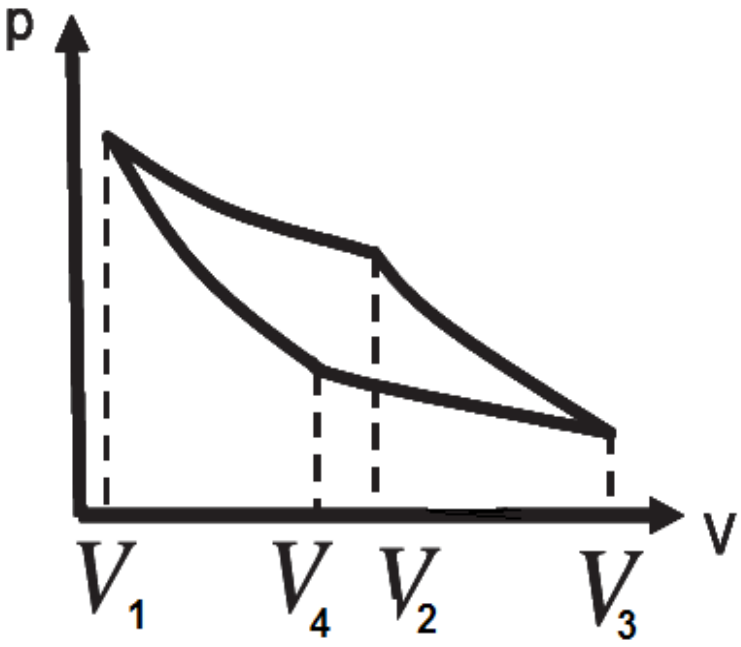

Figure 4.4: P-V diagram representing the four branches of Carnot-like cycle

The equation of state for the Van der waals gas is

$$(P + \frac{an^2}{V^2})(V - nb) = nRT \tag{4.1.14}$$

which can be rewritten, interms of molar volume, as

$$(P + \frac{a}{V_m^2})(V_m - b) = RT \tag{4.1.15}$$

where a and b are Van der Waals constants, P, V_m and T are pressure, molar volume and absolute temperature of the system, respectively. Adiabatic process of a gaseous system is governed by the following relation [64, 66]

$$V_m^{\gamma-1} \exp\left(\int \alpha(T)dT\right) = \text{constatnt} \tag{4.1.16}$$

where the coefficient of thermal expansion $\alpha(T)$ is defined as

$$\alpha(T) = \frac{1}{V}(\frac{\partial V}{\partial T})_P \tag{4.1.17}$$

The partial derivative of Van der waals equation with respect to T yields

$$(\frac{\partial}{\partial T})_P[(P+\frac{an^2}{V^2})(V-nb)] = (\frac{\partial}{\partial T})_P(nRT) \tag{4.1.18}$$

$$-\frac{2an^2}{V^3}(V-nb)(\frac{\partial V}{\partial T})_P + (P+\frac{an^2}{V^2})(\frac{\partial V}{\partial T})_P = nR \tag{4.1.19}$$

$$[\frac{nRT}{V-nb} - \frac{2an^2(V-nb)}{V^3}](\frac{\partial V}{\partial T})_P = nR \tag{4.1.20}$$

$$(\frac{\partial V}{\partial T})_P = \frac{nRV^3(V-nb)}{nRTV^3 - 2an^2(V-nb)^2} \tag{4.1.21}$$

Similarly

$$(\frac{\partial V}{\partial P})_T = \frac{V^3(V-nb)^2}{2an^2(V-nb)^2 - nRTV^3} \tag{4.1.22}$$

The coefficient of thermal expansion is then

$$\alpha(T) = \frac{1}{V}(\frac{\partial V}{\partial T})_P = \frac{nRV^2(V-nb)}{nRTV^3 - 2an^2(V-nb)^2} \tag{4.1.23}$$

To compute $\gamma - 1$ we can start from the first law of thermodynamics

$$dE = dQ - PdV \tag{4.1.24}$$

where E is total internal energy of the system, Q is heat energy flowing across the boundary of the system, P is pressure of the system and V is volume of the system. Letting E = E(T,V), we can write

$$dE = (\frac{\partial E}{\partial T})_V dT + (\frac{\partial E}{\partial V})_T dV \tag{4.1.25}$$

$$dQ - PdV = (\frac{\partial E}{\partial T})_V dT + (\frac{\partial E}{\partial V})_T dV \tag{4.1.26}$$

$$dQ = (\frac{\partial E}{\partial T})_V dT + [P + (\frac{\partial E}{\partial V})_T]dV \tag{4.1.27}$$

If the system is heated at constant volume, the change in the energy of the system is entirely due to the heat supplied, $dV = 0$. Hence specific heat of the system at constant volume is given by

$$C_V = (\frac{\partial Q}{\partial T})_V = (\frac{\partial E}{\partial T})_V \tag{4.1.28}$$

On the other hand specific heat of the system at constant pressure is given by

$$C_P = (\frac{\partial Q}{\partial T})_P = (\frac{\partial E}{\partial T})_V + [P + (\frac{\partial E}{\partial V})_T](\frac{dV}{dT})_P \tag{4.1.29}$$

$$C_P - C_V = [P + (\frac{\partial E}{\partial V})_T](\frac{dV}{dT})_P \tag{4.1.30}$$

From Hemholtz's equation [66]

$$(\frac{\partial E}{\partial V})_T = T^2(\frac{\partial}{\partial T}\frac{P}{T})_V = T(\frac{\partial P}{\partial T})_V - P \tag{4.1.31}$$

$$P + (\frac{\partial E}{\partial V})_T = T(\frac{\partial P}{\partial T})_V \tag{4.1.32}$$

$$C_P - C_V = T(\frac{\partial P}{\partial T})_V(\frac{\partial V}{\partial T})_P = T(\frac{\partial P}{\partial T})_V \alpha V \tag{4.1.33}$$

For three variables x = x(y,z), y = y(x,z) and z = z(x,y), the theory of functions of many variables define

$$(\frac{\partial x}{\partial y})_z(\frac{\partial y}{\partial z})_x(\frac{\partial z}{\partial x})_y = -1 \tag{4.1.34}$$

Hence we can define

$$(\frac{\partial P}{\partial T})_V(\frac{\partial T}{\partial V})_P(\frac{\partial V}{\partial P})_T = -1 \tag{4.1.35}$$

$$\begin{aligned}(\frac{\partial P}{\partial T})_V &= \frac{-1}{(\frac{\partial T}{\partial V})_P(\frac{\partial V}{\partial P})_T} \\ &= -\frac{(\frac{\partial V}{\partial T})_P}{(\frac{\partial V}{\partial P})_T} \\ &= \frac{-\frac{1}{V}(\frac{\partial V}{\partial T})_P}{\frac{1}{V}(\frac{\partial V}{\partial P})_T} \\ &= \frac{\alpha}{\kappa_T}\end{aligned} \tag{4.1.36}$$

where $\kappa_T = -\frac{1}{V}(\frac{\partial V}{\partial P})_T$ is isothermal compressibility. Thus eqn (4.1.33) becomes

$$C_P - C_V = T\alpha V(\frac{\alpha}{\kappa_T}) = \frac{TV\alpha^2}{\kappa_T} \tag{4.1.37}$$

$$\frac{C_P - C_V}{C_V} = \gamma - 1 = \frac{TV\alpha^2}{C_V\kappa_T} \tag{4.1.38}$$

Or in terms of molar volume

$$\gamma - 1 = \frac{TV_m\alpha^2}{C_V\kappa_T} \tag{4.1.39}$$

But the isothermal compressibility can be written as

$$\begin{aligned} \kappa_T &= -\frac{1}{V}(\frac{\partial V}{\partial P})_T \\ &= \frac{V^2(V-nb)^2}{nRTV^3 - 2an^2(V-nb)^2} \\ &= \frac{\alpha(V-nb)}{nR} \end{aligned} \tag{4.1.40}$$

$$\begin{aligned} \gamma - 1 &= \frac{TV\alpha^2}{nC_V\kappa_T} \\ &= \frac{TVnR\alpha^2}{nC_V\alpha(V-nb)} \\ &= \frac{TVR\alpha}{C_V(V-nb)} \\ &= \frac{TVR}{C_V(V-nb)}\frac{nRV^2(V-nb)}{nRTV^3 - 2an^2(V-nb)^2} \\ &= \frac{nTR^2V^3}{C_VnRTV^3 - 2an^2C_V(V-nb)^2} \end{aligned} \tag{4.1.41}$$

Integrating eqn (4.1.23) with respect to T yields

$$\int \alpha(T)dT = \ln[nRTV^3 - 2an^2(V-nb)^2]^{\frac{V-nb}{V}} + C \tag{4.1.42}$$

where C is integration constant.

$$\exp\int \alpha(T)dT = [nRTV^3 - 2an^2(V-nb)^2]^{\frac{V-nb}{V}} \exp C \tag{4.1.43}$$

$$V^{\gamma-1}\exp\int(\alpha(T)dT) = V^{\frac{nTR^2V^3}{C_VnRTV^3-2an^2C_V(V-nb)^2}}[nRTV^3 - 2an^2(V-nb)^2]^{\frac{V-nb}{V}} = \text{constatnt} \tag{4.1.44}$$

Or in terms of molar volume this can be written as

$$V_m^{\frac{TR^2V_m^3}{C_VRTV_m^3-2aC_V(V_m-b)^2}}[RTV_m^3 - 2a(V_m-b)^2]^{\frac{V_m-b}{V_m}} = \text{constatnt} \tag{4.1.45}$$

where a and b are Van der waals constants and R is universal gas constant. If the values for T_h, T_c, V_1 and V_3 are fixed, eqn (4.1.45) can be solved numerically to determine the values for V_2 and V_4.

4.2 Some Measurable Statistical Quantities

In Molecular Dynamics one can measure physical quantities of a given system simply by performing time averages of physical properties over the system trajectory. Physical properties are usually expressed as a function of coordinates and velocities of particles constituting the system. The physical quantities we measure while doing the simulation are the following.

4.2.1 Potential Energy

Potential energy U is a physical quantity associated with specific configuration of a system. Knowledge of U is required to verify energy conservation and to govern the dynamics of particles in the system. In our model only pair interaction is considered and we employ Lennard-Jones model [58 - 60] to compute the potential of the system.

$$U(\mathbf{r}_1, ..., \mathbf{r}_N) = \Sigma_i \Sigma_{j>i} V(\mid \mathbf{r}_i - \mathbf{r}_j \mid) \tag{4.2.1}$$

$$U_{LJ}(r) = 4\varepsilon[(\frac{\sigma}{r})^{12} - (\frac{\sigma}{r})^{6}] \tag{4.2.2}$$

4.2.2 Kinetic Energy

The instantaneous kinetic energy is given by

$$K(t) = \frac{1}{2} \sum_i m_i (v_i(t))^2 \tag{4.2.3}$$

Averaging the instantaneous value is straightforward.

4.2.3 Temperature

From equipartion theorem we know that each translational degree of freedom contibutes $\frac{1}{2} k_B T$ to the total average kinetic energy. Hence the average temperature of a system can be defined as

$$T = \frac{2K}{3Nk_B} \tag{4.2.4}$$

4.2.4 Pressure

Pressure of a system can be expressed as a function of independent parameters; temperature T and number density ρ, and hence the expression provide a link between microscopic and macroscopic parameters. Pressure, for the case of pair interaction, can be given by the following virial formula [60].

$$\begin{aligned} PV &= Nk_BT + \frac{1}{d}\sum_{i<j}\mathbf{r}_{ij}\cdot\mathbf{f}_{ij} \\ &= Nk_B\frac{2K}{3Nk_B} + \frac{1}{3}\sum_{i<j}\mathbf{r}_{ij}\cdot\mathbf{f}_{ij} \\ &= \frac{1}{3}[2K + \sum_{i<j}\mathbf{r}_{ij}\cdot\mathbf{f}_{ij}] \end{aligned} \tag{4.2.5}$$

where we have used average temperature $T = \frac{2K}{3Nk_B}$, since, in molecular dynamics simulation, where we consider microcanonical ensemble, energy, but not temperature, is constant. Thus pressure of a system becomes

$$P = \frac{\rho}{3N}[2K + \sum_{i<j}\mathbf{r}_{ij}\cdot\mathbf{f}_{ij}] \tag{4.2.6}$$

where K is average kinetic energy of the particles in the system and $\rho = \frac{N}{V}$ is number density.

Chapter 5

Results and Discussion

5.1 Heat Engine Operating With Constant Piston Speed Along Each Branch Of The Cycle

The model heat engine we consider for this study contains $N = 4000$ identical gas molecules in a cubic box of length $L = 50$ unit. The molar volume of the model system is 0.895 lt/mol which is small as compared to that of ideal gas, 22.414 lt/mol, and large enough as compared to that of water, 0.018 lt/mol. Hence we believe that the system is sufficiently concentrated to be considered as a system of real gas. We used the values of σ and ε for Ar to determine the molar volume of the model system. We start with the system of gas molecules initially configured with fcc lattice structure as shown in Fig. 5.1 and then let to melt by setting all the molecules to have initial velocity randomly selected from Maxwell-Boltzman distribution function and hence the gas molecules in the system have random arrangement where the system loss its geometric symmetry as shown in Fig. 5.2. The gas molecules are assumed to be similar point particles of equal mass $m = 1$ unit, in reduced unit. The other parameters that we used in reduced unit include Boltzman constant $k_B = 1$, the minimum value of Lennard Jones potential $\varepsilon = 1$, the interparticle separation at which Lennard Jones potential vanish $\sigma = 1$ and the temperature of the heat sink $T_c = 1.25$. In molecular dynamics simulation, especially when modelling fluids, it is convenient to work in dimensionless or reduced units. The advantages we experience in using such units include

- The possibility to work with numerical values of the order of unity, instead of the typically very small values associated with the atomic scale.
- The simplification of the equations of motion, due to the absorption of the parameters defining the model into the units.
- The possibility of scaling the results for a whole class of systems described by the same model.

All the above parameters remain the same in our all simulations. But we consider different values for the temperature of the heat source T_h and piston speed u. The process rate or piston speed is constant in any branch of the cycle, however its value in the isothermal branch is generally different from that of in the adiabatic branch. For this study we consider model engines operating at different piston speeds ranging from $u = 0.001$ to $u = 0.1$. These different process rates are considered only for the isothermal branches of the cycle, while the adiabatic processes performed at a uniform rate $u' = 0.01$ when $u > 0.01$ and $u' = 0.1$ when $u \leq 0.01$. This a relatively fast process rate on the adiabatic branches is considered to model the instant adiabatic process that usually exist in real heat engines. The reason for using two different process rates on the adiabatic branch, $u' = 0.01/0.1$, is as follow. The fastest possible process rate at which we obtain a T-V diagram for the cyclic process which is closer to that of Carnot cycle is when $u' = 0.01$ and hence we use, in our simulation, $u' = 0.01$ for all values of $u > 0.01$. However as the value for u further increases, we change the value of u' to 0.1 just to make sure that the process rate on the adiabatic branch is always larger than that of the isothermal one.

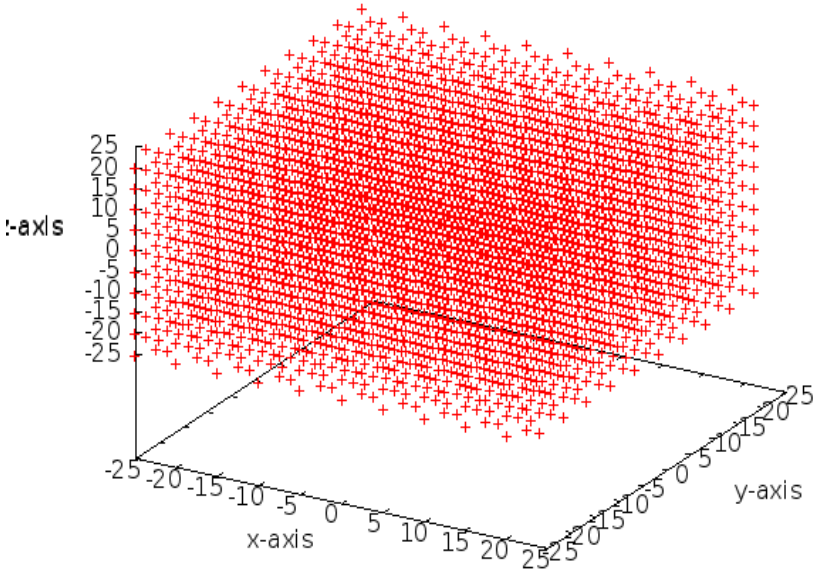

Figure 5.1: Initial configuration with fcc stracture

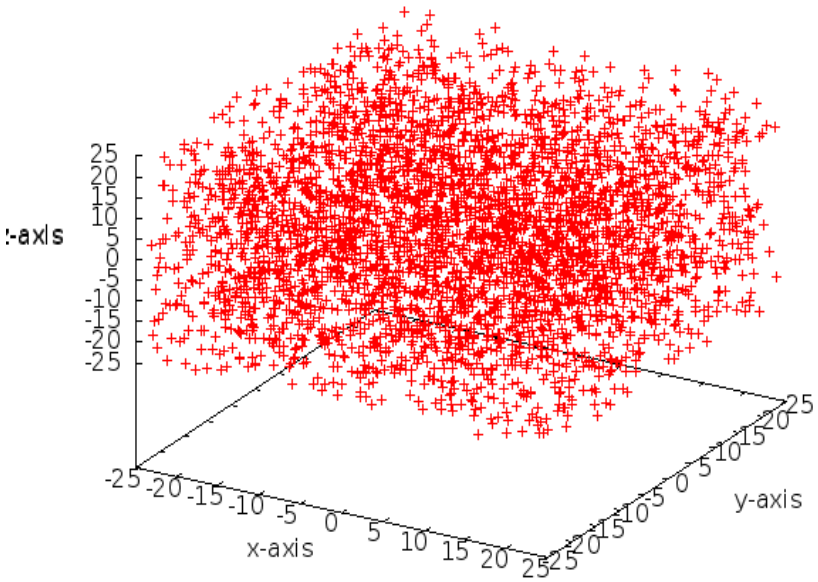

Figure 5.2: Configuration of the system after random initial velocities are assigned for all particles

The cyclic thermodynamic process in the working gas of a heat engine is studied for a heat engine model operating with a Carnot-like cycle between two heat reservoirs of temperature T_c and T_h. The working gas of the engine model is supposed to receive heat from the heat source at temperature T_h as it isothermally expands and reject heat to the heat sink at temperature T_c as it isothermally compressed. The isothermal expansion (compression) process is followed by adiabatic expansion (compression) proces which is takes place while the system is insulated, i.e. the working gas is disconnected from the reservoirs. This study includes the thermodynamic process taking place at different process rates, or piston speeds. The result obtained for $T_h = 1.65$ is discussed as follows. The variation of pressure with volume in the working gas is shown in Fig. 5.3. It is shown for both ideal and real gas system. For ideal gas we use the result obtained from analytical solution of $PV^{\gamma} = constant$, an expression satisfied by an ideal gas system undergoing adiabatic process. For real gas, however, we use the simulation result. The diagram shows the pressure of the system of real gas is almost similar to that of ideal gas at large volume as it is supposed to be, since for low concentration a system of real gas approximately behave as that of ideal gas. However, as the system is compressed the pressure of real gas system increases a bit faster than that of ideal gas system.

Fig. 5.4 shows the temperature-volume (T-V) diagram for the cyclic thermodynamic process performed by the working gas. The T-V diagram is ploted for both quasi-static process and the finite time process. For the quasi-static process the plot is obtained by using a constant temperature T_h in the isothermal expansion stage and a constant temperature T_c in the isothermal compression stage, while the adiabatic branch is plotted by using the result obtained from analytical solution of the well known relation $TV^{\gamma-1} = constant$ for adiabatic process in the system of ideal gas. Whereas for the finite-time process it is ploted using the result obtained from our simulation for three process rates $u = 0.1$, $u = 0.01$ and $u = 0.001$. As it is clearly seen on the diagram the curves representing adiabatic branches of the process are almost smooth, do not involve significant fluctuation as

it must be since at this stage the system is insulated, whereas in the isothermal branches there are small fluctuations which are in the order of or less than three percent and which is an acceptable and very common. As the process gets more slower and slower the T-V diagram more looks like that of Carnot cycle which evident that the model considered in this project approaches Carnot engine in the quasi-static limit.

The variation of efficiency with piston speed is represented in Fig. 5.5. The Carnot efficiency is very well realized for small piston speed values. The efficiency averaged over four complete cycles for piston speed u = 0.001 is obtained to be 0.211 which is very close to the Carnot efficiency $\eta_c = 0.242$. The variation of average power output per cycle with piston speed is shown in Fig. 5.6. As it can be seen from the graph the output power increases with piston speed until it reaches a maximum value and then starts to drop down. This shows that the power vanishes for both very slow and very fast processes. This is because, although there is a finite amount of work done for the slow proces, the time taken is very large so that the output power becomes vanishingly small. On the other hand when the process is fast the net average work done becomes very small and hence even if the time per cycle is also small the output power becomes very small. The output power reaches its maximum value when the piston speed is arround u = 0.01 and the corresponding efficiency is 0.113 which is very close to Curzon-Ahlborn efficiency $\eta_{CA} = 0.130$.

The value for optimum efficiency can be obtained by solving eqn (2.5.7) and determining the piston speed at which the objective function attains maximum value. In solving the problem we use the simulation data for average efficiency and average power output per cycle as a function of piston speed. It is solved for the entire range of piston speed where as the values for maximum and minimum efficiencies are taken to be Carnot efficiency and zero respectively. The plot for the objective function as a function of piston speed is shown in Fig. 5.7. The objective function attains its maximum value at piston

speed u = 0.0018. The efficiency of the engine model considered operating with this piston speed is $\eta_{opt} = 0.202 = 0.835\eta_c$. This value, called optimum efficiency, lies between Carnot efficiency and efficiency at maximum power. The corresponding value for power output per cycle, called optimum power, is obtained to be $P_{opt} = 0.523P_{max}$ where P_{max} is the maximum power output obtained.

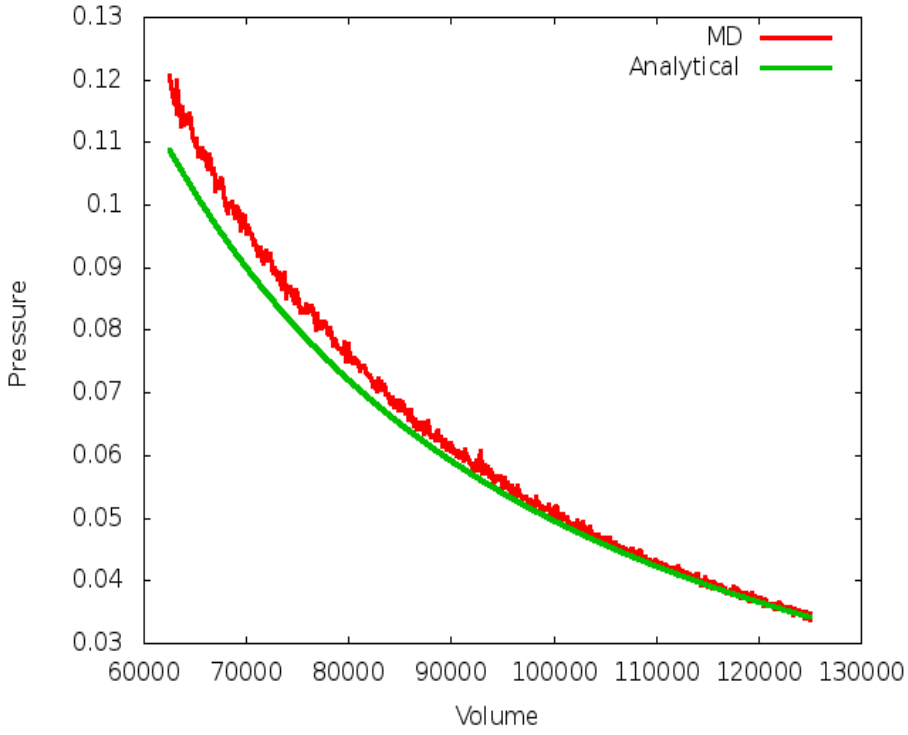

Figure 5.3: P-V diagram for adiabatic process when $T_h = 1.65$

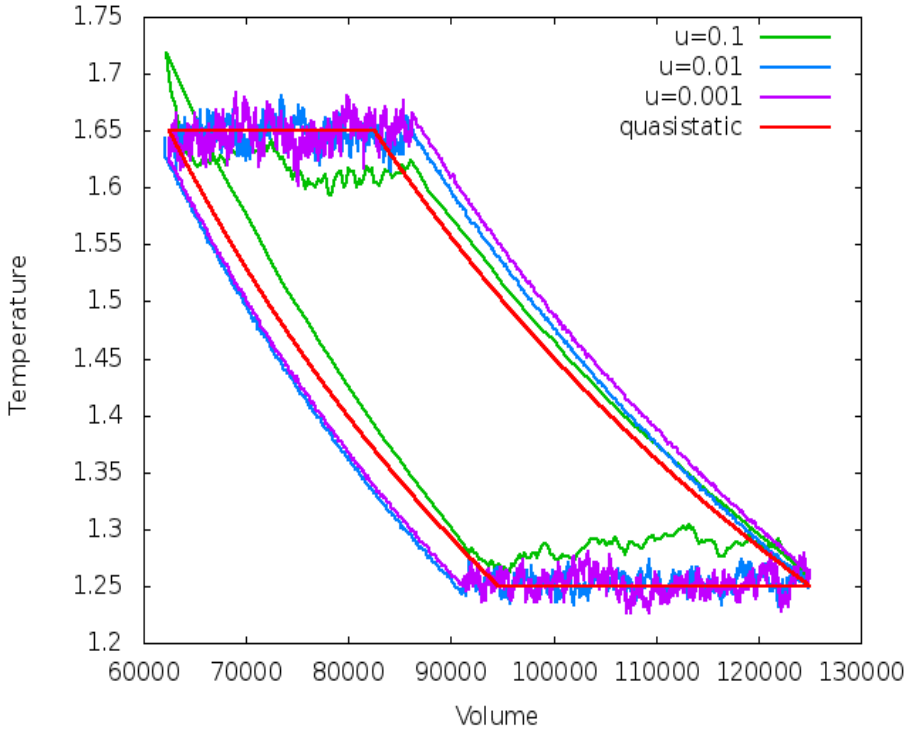

Figure 5.4: T-V diagram when $T_h = 1.65$

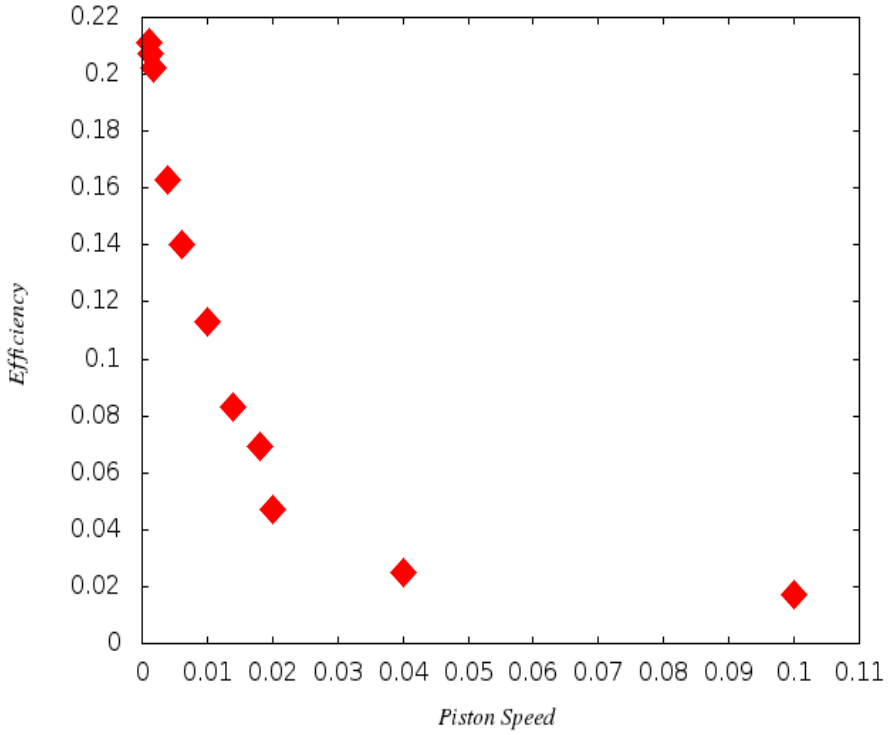

Figure 5.5: Efficiency-Piston speed diagram when $T_h = 1.65$

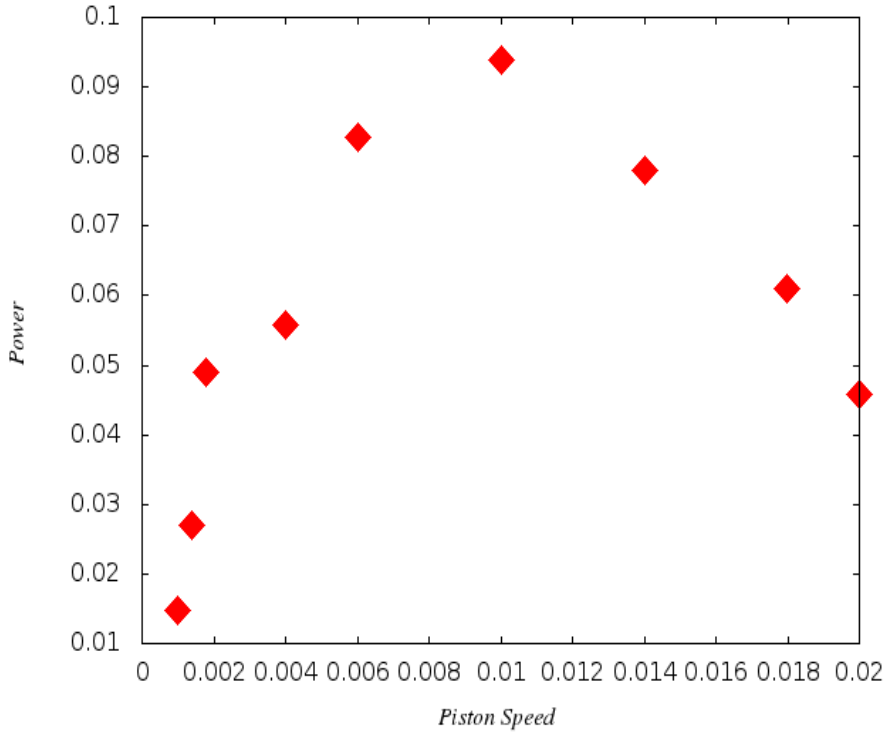

Figure 5.6: Power-Piston speed diagram when $T_h = 1.65$

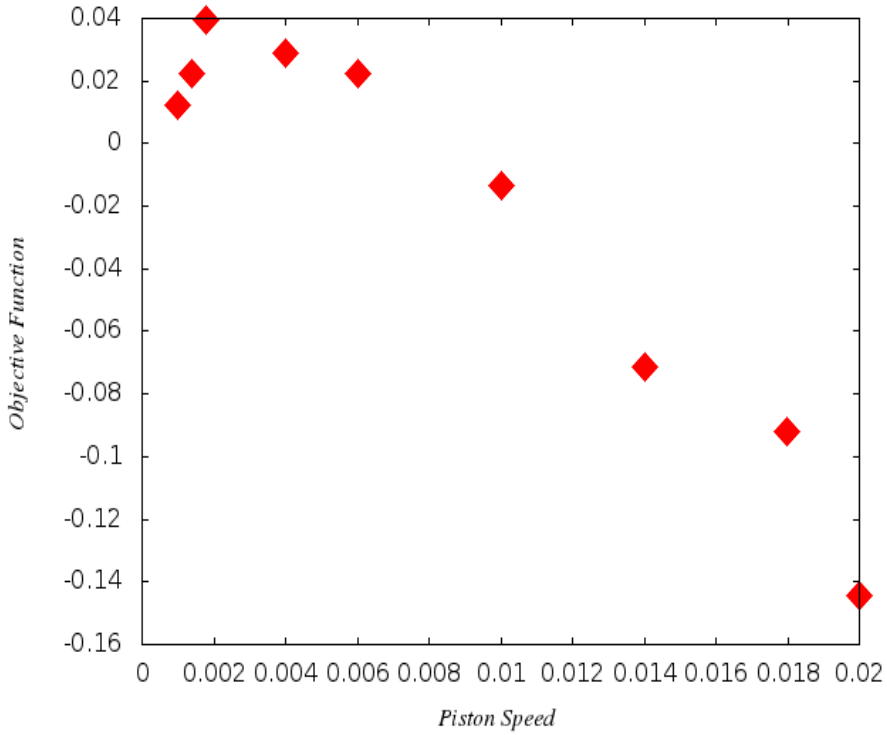

Figure 5.7: Objective function as a function of piston speed for $T_h = 1.65$

We did the same for all other considered values of T_h, $T_h = 1.45, 1.55, 1.75$ keeping constant $T_c = 1.25$. The T-V diagrams obtained for these T_h values looks like Fig. 5.4 except the curves representing the isothermal expanssion branches lay at the corresponding T_h values. The P-V diagrams are also obtained for all considered values of T_h following the same procedure stated above for $T_h = 1.65$ and we have seen that they are similar to Fig. 5.5 except that the peak value of the curve increases with T_h. Fig. 5.8 shows the variation of efficiency with piston speed for all values of T_h. As it can be clearly seen from the diagram as the piston speed increases efficiency decreases to vanishingly small value irrespective of the value of T_h. However, the maximum efficiency which is obtained for the smallest considered process rate varies for different values of T_h and actually it increases as T_h increases. The variation of average power output per cycle with piston speed for all values of T_h is shown in Fig. 5.9. In this figure it is shown that the power output vanishes for both very slow and very fast processes and attains a maximum value

for particular piston speed. The values for maximum efficiency and efficiency at maximum power obtained from our simulation for all considerd values of T_h are in good agreement with the corresponding values for Carnot efficiency and Curzon-Ahlborn efficiency. Fig. 5.10 shows the variation of efficiency with ratio of temperature of heat sink to that of heat source. It is shown that efiiciency decreases as the ratio T_c/T_h increases. Moreover we could compare the variation of efficiency with the ratio for different process rates and the obtained result assures that as the process get slower and slower the result approaches that of quasistatic process. The same figure asserts the linear dependency of efficiency on the temperature ratio which is in line with the theoretical formulation of Carnot efficiency, where it is shown that η_c depends only on the ratio $\frac{T_c}{T_h}$. Finally We compute optimum values for efficiency and power output per cycle following the same procedure stated above. The variation of the objective function with piston speed is presented in Fig. 5.11. The obtained results for optimum efficiency well lies between η_c and η_{CA}. The results obtained from the simulation for maximum efficiency, efficiency at maximum power, optimum efficiency and optimum power output per cycle are summarised in Table 5.1.

Table 5.1: Summary of main results obtained from the simulation for the engine model operating with constant but unequal piston speed along each branch of the cycle

T_h	η_{max}	$\eta_{P_{max}}$	η_{opt}	P_{opt}
1.45	$0.121 = 0.877\eta_c$	$0.074 = 1.027\eta_{CA}$	$0.108 = 0.783\eta_c$	$0.614P_{max}$
1.55	$0.172 = 0.887\eta_c$	$0.083 = 0.814\eta_{CA}$	$0.165 = 0.851\eta_c$	$0.449P_{max}$
1.65	$0.211 = 0.872\eta_c$	$0.113 = 0.869\eta_{CA}$	$0.202 = 0.835\eta_c$	$0.523P_{max}$
1.75	$0.268 = 0.937\eta_c$	$0.129 = 0.832\eta_{CA}$	$0.253 = 0.885\eta_c$	$0.492P_{max}$

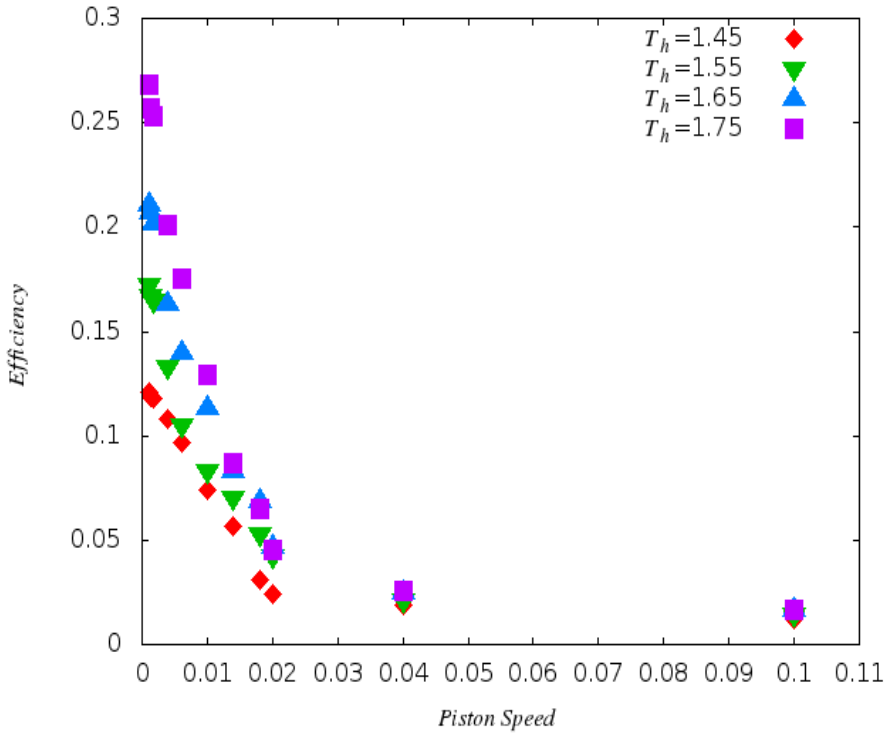

Figure 5.8: Efficiency-Piston speed diagram for the cyclic process performed at unequal piston speed

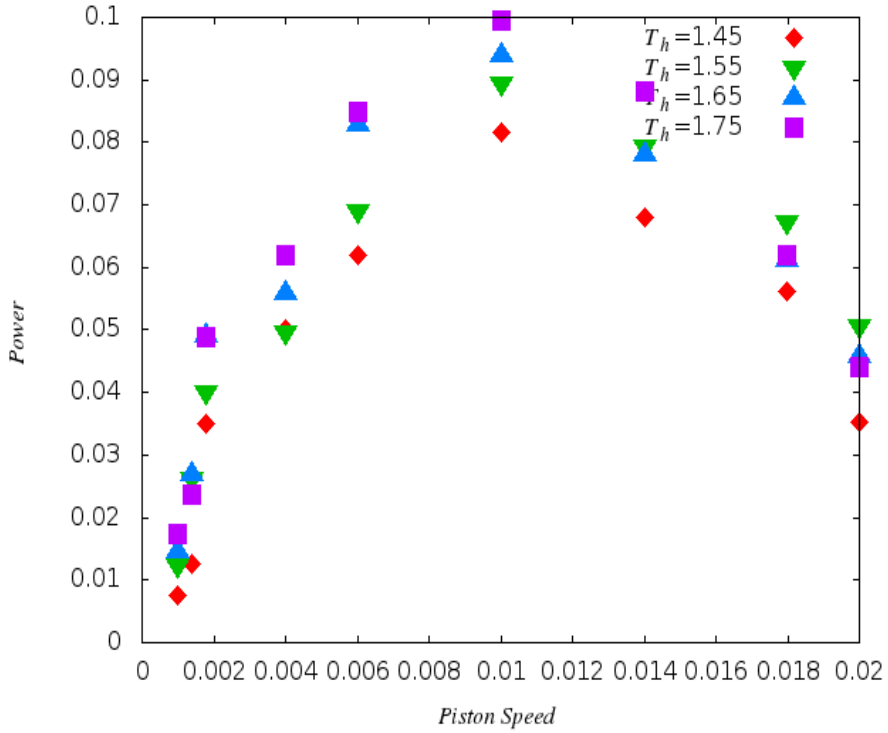

Figure 5.9: Power-Piston speed diagram for the cyclic process performed at unequal piston speed

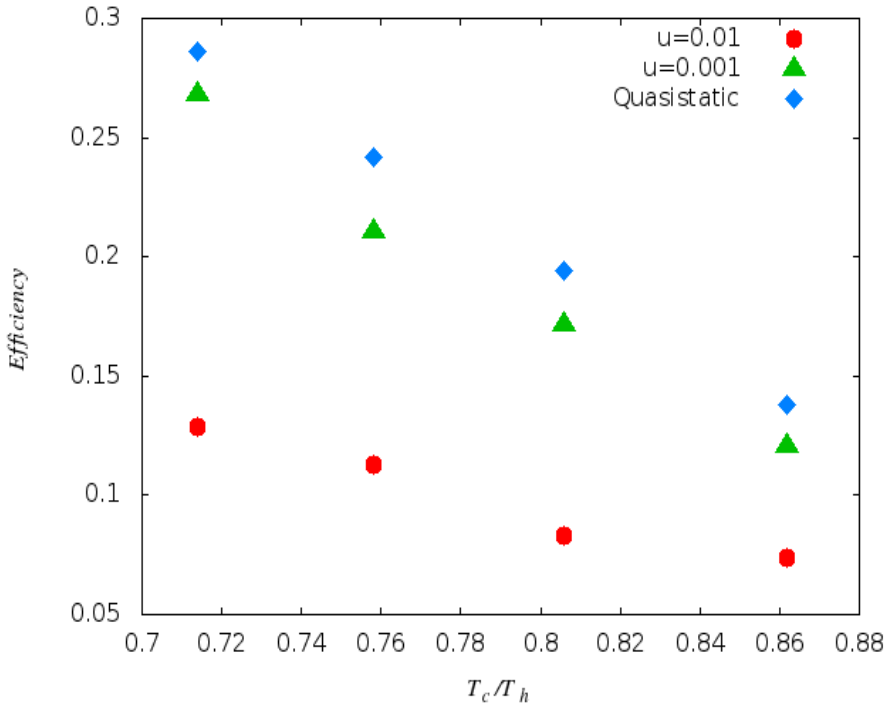

Figure 5.10: Efficiency-temperature ratio diagram for different process rates for the cyclic process performed at unequal piston speed

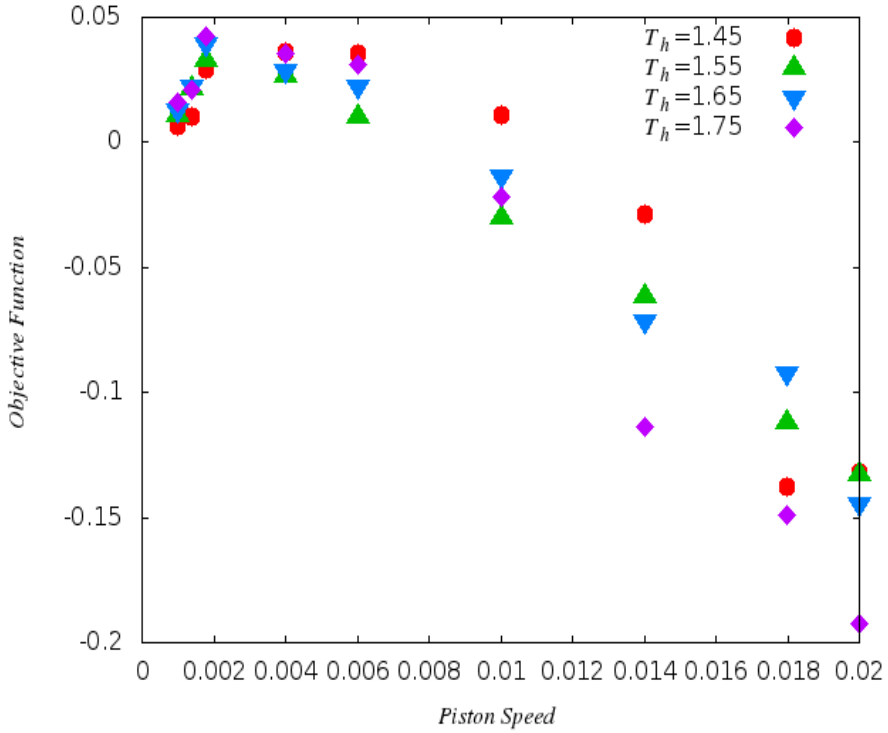

Figure 5.11: Objective function - Piston speed diagram for the cyclic process performed at unequal piston speed

5.2 Heat Engine Operating With Constant Process Rate Throughout The Cycle

We still consider a heat engine model containing $N = 4000$ identical gas molecules in a cubic box of length $L = 50$ unit. The gas molecules are assumed to be similar point particles of equal mass of $m = 1$ unit. The other parameters that we used in reduced unit include Boltzman constant $k_B = 1$, the minimum value for Lennard Jones potential $\varepsilon = 1$, the intermolecular separation at which Lennard Jones potential vanish $\sigma = 1$ and the temperature of the heat sink $T_c = 1.25$.

All the above parameters remain the same in our all simulations. But we consider different values for the temperature of the heat source T_h and piston speed u. The process rate or piston speed is constant throughout the cycle, i.e., unlike that of the previous section here we consider a model involving adiabatic and isothermal processes operating at the same rate. This model engine too studied for different piston speeds ranging from $u = 0.001$ to $u = 0.1$.

Except considering constant process rate throughout the complete cycle, all other parameters related to the system model and the steps of the cyclic process considered are exactly similar to what is considered in section 5.1. As a consequence the T-V and P-V diagrams showing the simulation result of the cyclic process for each values of T_h are obtained to be similar to that of what is obtained in the previous section for corresponding T_h values. From our simulation result we found that only the values related with efficiency and power output per cycle are deviate from the results of the previous section. Hence, to avoid unneccessary repetition, only the results related to these variables are discussed in this section.

The thermodynamic process in the working gas of the engine model is studied following the same procedure as that of the previous section for all considered values of T_h, $T_h =$ 1.45, 1.55, 1.65 and 1.75 keeping $T_c = 1.25$ constant. The variation of efficiency with piston speed for all considered values of T_h is presented in Fig. 5.12. It is shown in

the diagram that as the piston speed increases efficiency decreases to vanishingly small value irrespective of the value of T_h. However, the maximum efficiency which is obtained for the smallest considered process rate varies for different values of T_h and actually it increases as T_h increases. The variation of average power output per cycle with piston speed for all values of T_h is shown in Fig. 5.13. From this figure we can see that the power output vanishes for both very slow and very fast processes and attains a maximum value for particular piston speed. The values for maximum efficiency and efficiency at maximum power obtained from our simulation for all considerd values of T_h are less than the corresponding values that obtained in the previous section. This implies that a heat engine can perform with better efficiency if it is operating in such a way that the adiabatic process is faster than the isothermal one, i.e. considering instant adiabatic process can play a significant role in enhancing efficiency of a heat engine. Fig. 5.14 shows the variation of efficiency with ratio of temperature of heat sink to that of heat source. It is shown that efiiciency decreases as the ratio T_c/T_h increases. Moreover we could compare the variation of efficiency with the ratio for different process rates and it is shown that a heat engine operating at a slower process rate perform with a much better efficiency than that of operating at a faster process rate. The same figure asserts the linear dependency of efficiency on the temperature ratio which is in line with the theoretical formulation of Carnot efficiency, where it is shown that η_c depends only on the ratio $\frac{T_c}{T_h}$. Finally We compute optimum values for efficiency and power output per cycle following the same procedure stated in the previous section. Fig. 5.15 shows that the objective function attains its maximum for a particular piston speed which is taken to be the optimum path for the cyclic thermodynamic process which delivers optimum efficiency and power output per cycle of the engine. The obtained results for optimum efficiency well lies between η_c and η_{CA}. The results obtained from the simulation for maximum efficiency, efficiency at maximum power, optimum efficiency and optimum power output per cycle are summarised in Table 5.2.

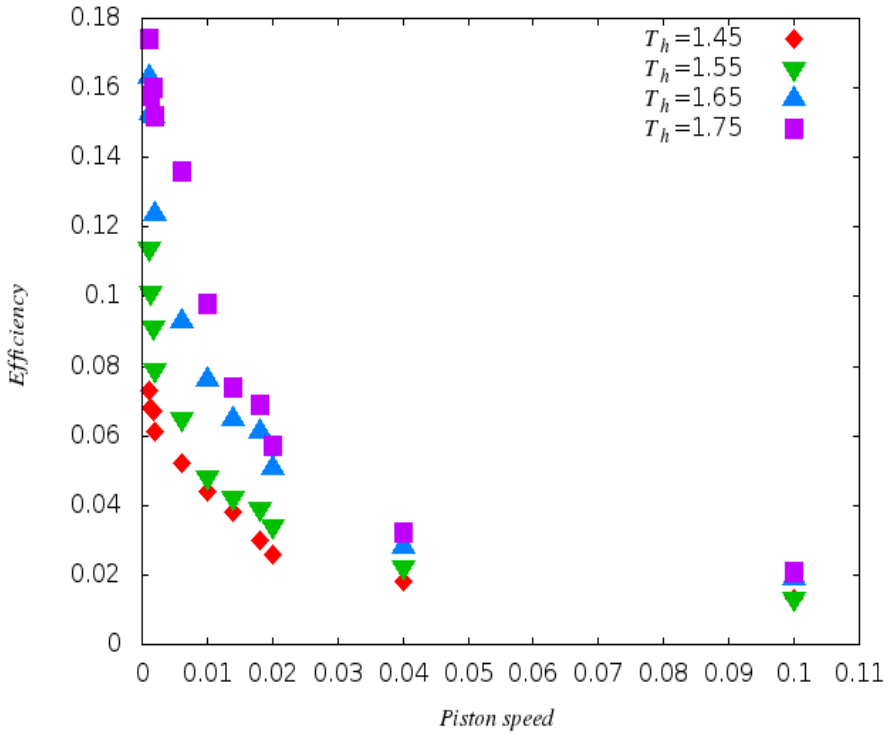

Figure 5.12: Efficiency-Piston speed diagram for the cyclic process performed at constant piston speed

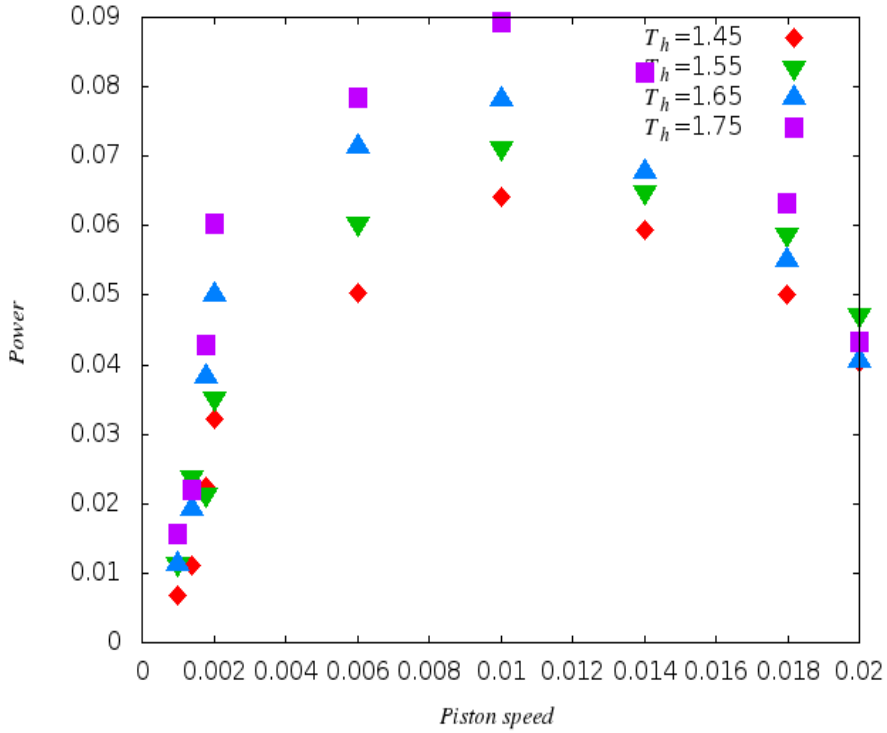

Figure 5.13: Power-Piston speed diagram for the cyclic process performed at constant piston speed

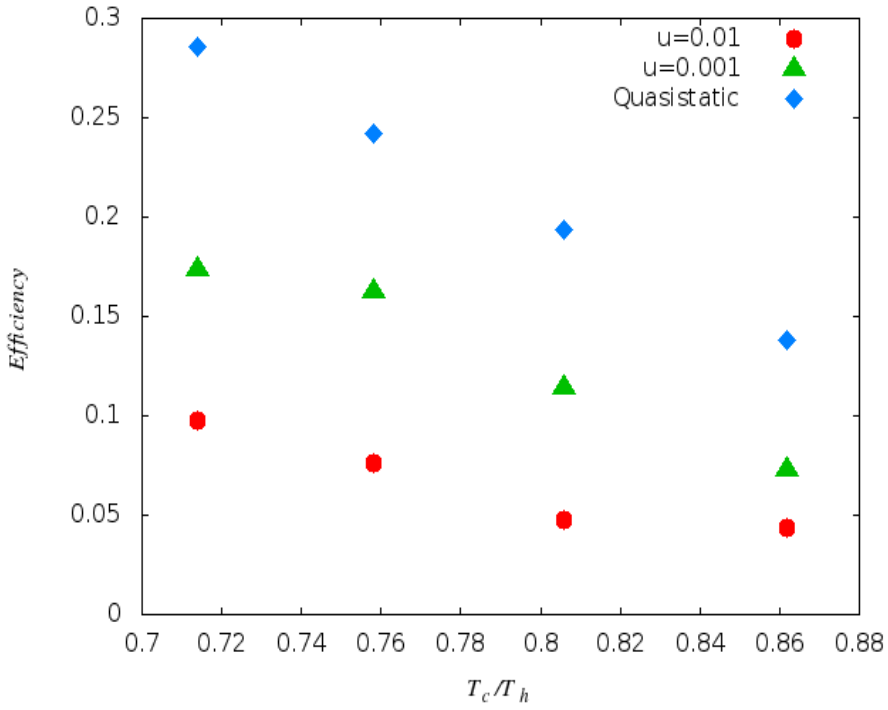

Figure 5.14: Efficiency-temperature ratio diagram for different process rates for the cyclic process performed at constant piston speed

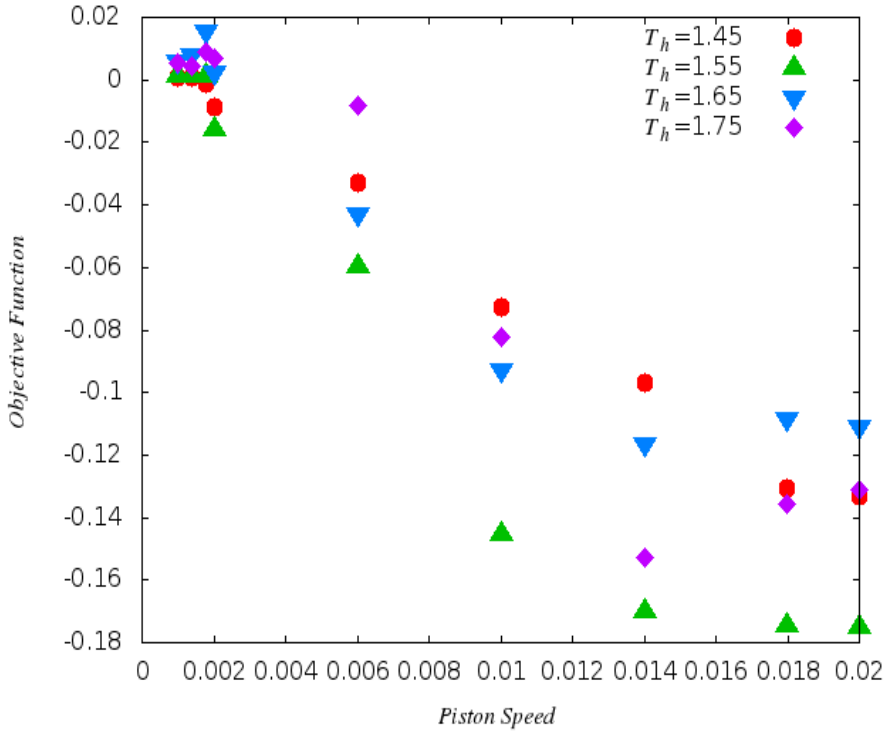

Figure 5.15: Objective function - Piston speed diagram for the cyclic process performed at constant piston speed

Table 5.2: Summary of main results obtained from the simulation for the engine model operating with constant piston speed throughout the cycle

T_h	η_{max}	$\eta_{P_{max}}$	η_{opt}	P_{opt}
1.45	$0.073 = 0.529\eta_c$	$0.044 = 0.611\eta_{CA}$	$0.071 = 0.514\eta_c$	$0.245P_{max}$
1.55	$0.114 = 0.588\eta_c$	$0.048 = 0.471\eta_{CA}$	$0.099 = 0.510\eta_c$	$0.469P_{max}$
1.65	$0.163 = 0.674\eta_c$	$0.076 = 0.585\eta_{CA}$	$0.152 = 0.628\eta_c$	$0.490P_{max}$
1.75	$0.174 = 0.608\eta_c$	$0.098 = 0.632\eta_{CA}$	$0.160 = 0.599\eta_c$	$0.480P_{max}$

Chapter 6

Summary and Conclusion

We perform 3D classical molecular dynamics simulation to calculate the average values for the measurable quantities of the system, such as temperature of the working gas as a function of volume, efficiency per cycle and power out put per cycle of the model engine as a function of process rate (piston speed) and pressure as a function of volume. All these quantities are taken to be averaged over 4 - 10 complete cycles. The temperature versus volume (T-V) diagram is ploted for both quasi-static process and the finite time process. T-V diagram for the finite-time process is ploted using the average result obtained from our simulation where as for the quasi-static process the plot is obtained by using a constant temperature T_h in the isothermal expansion stage and a constant temperature T_c in the isothermal compression stage, while the adiabatic branch is plotted by using the result obtained from analytical solution of the relation $TV^{\gamma-1} = constant$.

In this work we consider a model of heat engine whose working substance is real gas enclosed in a cubic box of length $L = 50$ unit. We consider a real gas system containing 4000 identical gas molecules of mass $m = 1$ unit. Intermolecular interaction is considered through employing the shifted Lennard-Jones potential where long range interaction is neglected. The thermodynamic process in the system follows four steps to complete one Carnot-like cyle; isothermal expansion, adiabatic expansion, isothermal compression and adiabatic compression. The expansion and compression steps of the cyclic process in the system is performed by setting the piston, one side of the cubic box, to move back and

forth at specific speed. In the first step the system expands doing work against the piston while the temperature kept constant. In this step the system is set to be in thermal contact with a constant energy supply, a heat reservior at temperature T_h, which ensures constant temperature of the system through out the process. In the second step the system continue expanding doing work against the piston but with out any heat exchange. In this step the system disconnected from the heat reservior and hence the adiabatic expansion stage keep on reducing the temperature of the system, as a result of loosing energy while doing work against the piston, until it attains the lowest temperature T_c. Once the system attains this lowest temperature the expansion stage of the cyclic process ends and followed by the compression stage where the piston turns to move in the opposite direction. The third step is then the isothermal compression stage where the system get compressed while it is in thermal contact with a heat reservior at temperature T_c which ensures the temperature of the system remains constant. The cycle of the process concluded by performing adiabatic compression. During this process the system disconnected from the reservior and the compression continue until the system attains its initial volume (the volume of the system before the first expansion starts) where it attains its initial temperature T_h too. These four processes all together form one complete cycle and the process can be repeated for the desired number of complete cycles depending up on the process rate. We consider higher number of complete cycles for the faster process than that of the slower process. This is done to average the measured values over larger number of complete cycles for the faster process than the slower process since fluctuation is a bit higher in the former case.

We have calculated average values for the measurable quantities we are interested on, such as efficiency and power output per cycle. We have seen that the efficiency approaches Carnot efficiency for slower process, small piston speed, while it approaches zero when the process rate, or piston speed, becomes higher. We have also obtain that the power output per cycle increases with the process rate until it attains a maximum value for particular

process rate and then starts to decrease and approches zero. The values for efficiency at maximum power are also computed for each of considered values of T_h and the obtained result is in a good agreement with theoretical values of η_{CA}. The other interesting result we obtain from our study is the optimum values for efficiency and power output per cycle. These values are computed by applying the unified optimization criterion developed by A. C. Hernandez and his colleagues for any energy converter [51]. The objective function is developed in such a way that it can let to obtain the optimum path that can make best compromise between effective useful energy and lost useful energy. As we can notice from eqn (2.5.7) the objective function explicitly depend on power which inturn depend on piston speed which is taken to be independent parameter in our model since it is easily controlable. After following the variation of the objective function with piston speed we found that the objective function attains its maximum for one particular value of piston speed in the allowed parameters(efficiency and piston speed) range. The value of the independent parameter at which the objective function attains maximum value is then taken to be the optimum path the thermodynamic process in the working gas need to follow to make the best compromise between effective useful energy and lost useful energy. We could also identify the optimum path for our model for all values of T_h considered.

- We develope a performance analysis method by applying classical MD simulation technique for heat engine operating with Carnot-like cycle and use real gas as the working substance.

- We study performance analysis of heat engine whose working substance is real gas.

- We apply 3D classical MD simulation technique for the first time to study the thermodynamic processes in the working gas of heat engine.

- The behaviour of the heat engine model we considered approaches the behaviour of the quasistatic Carnot cycle for small process rate. This is well demonstrated on

the T-V diagrams where we have seen that the T-V diagram for finite-time process approaches that of quasistatic process for small piston speed value.

- The efficiency of the heat engine model we consider approaches Carnot efficiency for small piston speed value.

- The average power out put per cycle of the engine exhibits a maximum value for some process rate and decrease to vanishingly small value in both directions.

- We determine the values for maximum efficiency and efficiency at maximum power and the obtained result is in a good aggreement with the theoretical result for η_c and η_{CA} respectively.

- The optimum path for the cyclic thermodynamic process which gives the best compromize between effective useful energy and lost useful energy is identified by applying unified optimization criterion.

- Optimum values for efficiency and power output per cycle are also determined. We found that the optimized efficiency well lies between maximum efficiency and efficiency at maximum power.

- The variation of efficiency of a heat engine with temperature ratio $\frac{T_c}{T_h}$ is considered in this study and we demonstrate that efficiency significantly decrease as the ratio increases. It is also shown that the efficiency versus temperature ratio curve for small process rate approaches that of the theoretical result for quasistatic process.

- It is also shown that considering instant process in the adiabatic branches (process taking place at a high rate in the adiabatic branches as compared to that of in the isothermal branches) of the cyclic process can significantly enhance the efficiency of the engine.

Bibliography

[1] S. Carnot, Reflexions sur la Puissance Motrice du Feu, et sur les Machines Propres a‘ Developper cette Puissance (1824).

[2] H.T. Odum and R.C. Pikerton, Am. Sc. **43**, 331 (1955).

[3] F. Curzon and B. Ahlborn, Am. J. Phys. **43**, 22 (1975).

[4] I. I. Novikov, At. Energy (N.Y.) **3**, 1269 (1957).

[5] I. I. Novikov, J. Nucl. Energy **7**, 125 (1958).

[6] P. Chambadal, Les centrales nucleaires (Armand Colin, 1957).

[7] H. S. Leff, Am. J. Phys **55**, 602 (1987).

[8] J. Gordon, Am. J. Phys **57**, 136 (1989).

[9] Rahim Ebrahimi, Report and Opinion **1**, 25 (2009), http://www.sciencepub.net/report

[10] Junxing Lin, Lingen Chen, Chih Wu and Fengrui Sun, Int. J. Energy Res., **23**, (1999)

[11] H. B. Callen, Thermodynamics and an Introduction to Thermostatistics, Wiley, 2nd ed., (1985).

[12] H. Feng, L. Chen and F. Sun, Rev.Mex.Fis. **56**, 135 (2010)

[13] D. C. Agrawal and V. J. Menon, Eur. J. Phys. **30**, 295 (2009)

[14] E. Rebhan, Am. J. Phys. **70**, 11 (2002)

[15] G. Aragon-Gonzalez et al., Brazilian Journal of Physics **38**, 4, (2008)

[16] J. Chen et. al, Energy Conversion and Management **42**, 173 (2001)

[17] M. Esposito et. al., arXiv:1008.2464v2 [cond-matt-stat-mech] (2010)

[18] J. Chen, J. Phys. D: Appl. Phys. **27**, 1144 (1994)

[19] A. Bejan, J. Appl. Phys. **79**, 1191 (1996)

[20] L. Chen, F. Sun, C. Wu, J. Inst. Energy **70**, 2 (1997)

[21] C. Y. Cheng, C. K. Chen, Energy Sources **19**, 461 (1997)

[22] R. Y. Nuwayhid, F. Moukalled and F. Noueihed, Energy Convers. Manag. **41**, 891 (2000)

[23] S. C. Kaushik, P. Kumar, Ind J Pure Appl Phys **39**, 628 (2001)

[24] B. Sahin, A. Kodal and H. Yavuz, J. Phys. D: Appl. Phys. **29**, 1162 (1996)

[25] G. Maheshwari, A. I. Khandwawala and S. C. Kaushik, Int. J. Ambient Energy **26**, 71 (2005)

[26] T. Yimaz, J. Energy Inst. **79**, 38 (2006)

[27] G. Maheshwari, S. Chaudhary and S. K. Somani, Int. J. Low-Carbon tecnol **4**, 9 (2009)

[28] T. Schmeidl and U. Seifert, Euro. phys. Lett. **81**, 20003 (2008)

[29] M. Esposito, K. Lindenberg and C. Van den Broeck, phys. Rev. Lett. **102**, 130602 (2009)

[30] M. Esposito, R. Kawai, K. Lindenberg and C. Van den Broeck, phys. Rev. Lett. **105**, 150603 (2010)

[31] Y. Apertet, H. Ouardane, C. Goupil and P. H. Lecoeur, arXiv:1111.1619v1 [cond-matt-stat-mech] (2011)

[32] Y. Izumida and K. Okuda, EPL **83**, 60003 (2008)

[33] Giuliano Benenti, Keiji Saito and Giulio Casati, arXiv:1102.4735v1 [cond-matt-stat-mech] (2011)

[34] D. Ladino-Luna, Rev.Mex.Fis. **48**, 6 (2002)

[35] L. Chen, S. Xia and F. Sun, Revista Mexicana Defisica, **56**, 231 (2010)

[36] Jun Li, Lingen Chen and Fengrui Sun, Pramana - J. Phys., **74**, 2 (2010)

[37] http://ffden-2.phys.uaf.edu

[38] http://www.fueleconomy.gov

[39] Kalyan Annamalai and Lshwar K. Puri, *Adnanced Thermodynamics Engineering*, CRC press (2002)

[40] http://www.kshitij-school.com

[41] P. Salamon, B. Andresen and R. S. Berry, Phys. Rev. A, **15**, 2094 (1977).

[42] P. Salamon and A. Nitzan, J. Chem. Phys. **74**, 3546 (1981)

[43] P. Salamon, A. Nitzan, B. Andresen, and R. S. Berry, Phys. Rev. A **21**, 2115 (1980)

[44] E. Rebhan and B. Ahlborn, Am. J. Phys., **55**, 423 (1987)

[45] Angulo-Brown F., J. Appl. Phys. **69**, 11 (1991)

[46] Shiyan Zheng, Guoxing Lin, Front. Energy Power Eng. China, **4**, 4 (2010)

[47] Mozurkewich M, Berry R., Proc. Natl. Acad. Sci USA, **78**, 4 (1981)

[48] Mozurkewich M, Berry R., Journal of Applied Physics, **53**, 1 (1982)

[49] Yan Zijun., J. Appl. Phys. **73**, 7 (1991)

[50] Cheng Ching-Yang, Chen Chao-Kung, J. Phys. D: Appl Phys, **30**, 1 (1997)

[51] A. C. Hernandez, A. Medina, J. M. M. Roco, J. A. White and S. Velsaco, Phys. Rev. E, **63**, 037102 (2001)

[52] Mehari Bayou and Mulugeta Bekele, MSc. Thesis Addis Ababa University, Addis Ababa (2010) (Unpublished)

[53] A. Bandivadekar, K. Bodek, L. Cheah, et.al., *On the Road in 2035:Reducing Transportations Petroleum Consumption and GHG Emissions*, Massachusetts Institute of Technology (2008).

[54] G. J. Snyder and E. S. Toberer, Nature Materials, **7**, 105 (2008)

[55] M. P. Allen, *Introduction to Molecular Dynamics Simulation*, John von Neumann Institute for Computing, **23** (2004)

[56] Furio Ercolessi, *A Molecular Dynamics Primer*, http://www.sissa.it

[57] D. Frenkel, B. Smit. *Understanding Molecular Simulation: From Algorithms to Applications*, 2nd Edition, Academic Press, London (2002).

[58] M. P. Allen and D.J. Tildesley, *Molecular Dynamics Simulation of Liquids*, Oxford University Press Inc. (1987)

[59] J. M. Haile, *Molecular Dynamics Simulation*, John Wiley and Sons Inc. (1992)

[60] D. C. Rapaport, *The Art of Molecular Dynamics Simulation*, Cambridge University Press (1995)

[61] D. Tabor, *Gases, Liquids, and Solids, and other states of matter*, 3rd Edition, Cambridge Univ. Press (1991).

[62] F. Reif, *Fundamentals Of Statistical And Thermal Physics*. McGraw-Hill Inc., (1965)

[63] Raymond A. Serway and John W. Jewet, *Physics For Scientists And Engineers*, Thomson Brooks/Cole, 6th ed. (2004)

[64] D. Kondepudi and I. Prigogine, Modern Thermodynamics, Wiley, 3rd ed. (2002)

[65] J. L. Xu, Z. Q. Zhou, J. Heat Mass Transf, **40** (2004)

[66] L. E. Reichl, *A Modern Course In Statistical Physics*, John Wiley and Sons, Inc., 2nd ed. (1998)

[67] H Gould and J. Tobochnik, *Statistical And Thermal Physics: With Computer Applications*, Princeton University Press (2010)

Declaration

This thesis is my original work, has not been presented for a degree in any other University and that all the sources of material used for the thesis have been dully acknowledged.

Name: **Kumneger Tadele**

Signature:

Place and time of submission: Addis Ababa University, April 2014

This thesis has been submitted for examination with our approval as University supervisors.

Name: **DR. MULUGETA BEKELE**

Signature:

Name: **DR. TATEK YERGOU**

Signature: